PERFORMANCE OPTIMIZATION OF MARIB GAS TURBINES POWER PLANT INTEGRATED WITH ORGANIC RANKINE CYCLE AND ABSORPTION REFRIGERATION SYSTEM

2024
MASTER THESIS
MECHANICAL ENGINEERING

Marwan Nabil Mohammed AL-ARASHI

Thesis Advisor
Assist. Prof. Dr. Abdulrazzak Ahmed S. AKROOT

PERFORMANCE OPTIMIZATION OF MARIB GAS TURBINES POWER PLANT INTEGRATED WITH ORGANIC RANKINE CYCLE AND ABSORPTION REFRIGERATION SYSTEM

Marwan Nabil Mohammed AL-ARASHI

Thesis Advisor
Assist. Prof. Dr. Abdulrazzak Ahmed Saleh AKROOT

T.C.
Karabuk University
Institute of Graduate Programs
Department of Mechanical Engineering
Prepared as
Master Thesis

KARABUK
May 2024

I certify that in my opinion the thesis submitted by MARWAN NABIL MOHAMMED AL-ARASHI titled "PERFORMANCE OPTIMIZATION OF MARIB GAS TURBINES POWER PLANT INTEGRATED WITH ORGANIC RANKINE CYCLE AND ABSORPTION REFRIGERATION SYSTEM" is fully adequate in scope and in quality as a thesis for the degree of Master of Science.

Assist. Prof. Dr. Abdulrazzak Ahmed Saleh AKROOT .....

Thesis Advisor, Department of Mechanical Engineering

This thesis is accepted by the examining committee with a unanimous vote in the Department of Mechanical Engineering as a Master of Science thesis. May 29, 2024

Examining Committee Members (Institutions)	Signature
Chairman : Prof. Dr. Mehmet ÖZALP (KBU)	.....
Member : Assist. Prof. Dr. Aead M. Ahmed (UOM)	.....
Member : Assist. Prof. Dr. Abdulrazzak AKROOT (KBU)	.....

The degree of Master of Science by the thesis submitted is approved by the Administrative Board of the Institute of Graduate Programs, Karabuk University.

Assoc. Prof. Dr. Zeynep ÖZCAN .....

Director of the Institute of Graduate Programs

"I declare that all the information within this thesis has been gathered and presented in accordance with academic regulations and ethical principles and I have according to the requirements of these regulations and principles cited all those which do not originate in this work as well."

Marwan Nabil Mohammed AL-ARASHI

ABSTRACT

M. Sc. Thesis

PERFORMANCE OPTIMIZATION OF MARIB GAS TURBINES POWER PLANT INTEGRATED WITH ORGANIC RANKINE CYCLE AND ABSORPTION REFRIGERATION SYSTEM

Marwan Nabil Mohammed AL-ARASHI

Karabük University
Institute of Graduate Programs
The Department of Mechanical Engineering

Thesis Advisor:
Assist. Prof. Dr. Abdulrazzak Ahmed Saleh AKROOT
May 2024, 63 pages

This thesis investigates the development and performance analysis of an innovative hybrid power system designed for the Marib, Yemen region, incorporating a Brayton cycle (BC), an Organic Rankine Cycle (ORC), and an absorption refrigeration system (ARS). Aimed at optimizing operational standards and efficiency, the system is engineered to leverage waste heat recovery, thereby minimizing thermal losses, enhancing system efficiency, and reducing operational costs. Through a comprehensive 4E analysis—encompassing energy, exergy, economic, and environmental perspectives—this study evaluates the impact of various operational parameters on the system's performance, employing the Engineering Equation Solver (EES) for model creation. Key findings include a significant boost in net power output to approximately 189.6 MW upon ORC integration, alongside a notable refrigeration output of 35.8 MW at a coefficient of performance (COP) of 0.81. The energy and

exergetic efficiencies of the newly developed model are recorded at 38.9% and 40.16% respectively, compared to 30.19% and 31.27% for the Marib gas turbine power plant. Exergoeconomic analysis reveals that the unit cost of specific energy for the new model is 54.52 USD/GJ, whereas for the Marib plant, it stands at 63.62 USD/GJ. Environmental assessments indicate a decrease in the carbon footprint from 631 kg/MWh to 485.5 kg/MWh, underscoring the significant emission reduction potential of the newly developed system. Parameters related to the BC, notably the pressure ratio and gas turbine inlet temperature (GTIT), emerged as critical to the system's efficiency. The study confirms that strategic adjustments to these parameters can markedly improve hybrid power systems' economic and environmental performance.

Key Words : Hybrid Power System, Waste Heat Recovery, Energy and Exergy Analysis, Exergoeconomic Analysis., Environmental Impact, Marib -Yemen.

Science Code : 91436

ÖZET

Yüksek Lisans Tezi

ORGANİK RANKİNE ÇEVRİMİ VE ABSORPSİYONLU SOĞUTMA SİSTEMİ İLE ENTEGRE MARİB GAZ TÜRBİNLERİ ENERJİ SANTRALİ PERFORMANS OPTİMİZASYONU

Marwan Nabil Mohammed AL-ARASHI

Karabük Üniversitesi
Lisansüstü Eğitim Enstitüsü
Makine Mühendisliği Bölümü

Tez Danışmanı:
Dr. Öğr. Üyesi Abdulrazzak Ahmed Saleh AKROOT
Mayıs 2024, 63 sayfa

Bu tezde, Yemen'in Marib bölgesi için tasarlanan, Brayton çevrimi (BC), Organik Rankine Çevrimi (ORC) ve absorpsiyonlu soğutma sistemi (ARS) içeren yenilikçi bir hibrit güç sisteminin geliştirilmesini ve performans analizini incelenmiştir. Operasyonel standartları ve verimliliği optimize etmeyi amaçlayan sistem, atık ısı geri kazanımını güçlendirecek, böylece termal kayıpları en aza indirecek, sistem verimliliğini artıracak ve operasyonel maliyetleri azaltacak şekilde tasarlandı. Enerji, ekserji, ekonomik ve çevresel perspektifleri kapsayan kapsamlı bir 4E analizi aracılığıyla bu çalışma, model oluşturmak için Mühendislik Denklem Çözücüsünü (EES) kullanarak çeşitli operasyonel parametrelerin sistem performansı üzerindeki etkisini değerlendirir. Temel bulgular arasında, ORC entegrasyonu sonrasında net güç çıkışında yaklaşık 189,6 MW'a önemli bir artış ve 0,81 performans katsayısında (COP) 35,8 MW'lık dikkate değer bir soğutma çıkışı yer alıyor. Yeni geliştirilen modelin

enerji ve enerji verimliliği, Marib gaz türbini santrali için% 30,19 ve% 31,27'ye kıyasla sırasıyla% 38,9 ve% 40,16 olarak kaydedilmiştir. Eksergoekonomik analiz, yeni model için özgül enerjinin birim maliyetinin 54,52 USD / GJ olduğunu, Marib tesisi için ise 63,62 USD / GJ olduğunu ortaya koymaktadır. Çevresel değerlendirmeler, karbon ayak izinin 631 kg / mwh'den 485,5 kg / mwh'ye düştüğünü gösteriyor ve bu da yeni geliştirilen sistemin önemli emisyon azaltma potansiyelinin altını çiziyor. BC ile ilgili parametreler, özellikle basınç oranı ve gaz türbini giriş sıcaklığı (GTIT), sistemin verimliliği için kritik olarak ortaya çıktı. Çalışma, bu parametrelerdeki stratejik ayarlamaların hibrit güç sistemlerinin ekonomik ve çevresel performansını belirgin şekilde iyileştirebileceğini doğrulamaktadır.

Anahtar Kelimeler : Hibrit Güç Sistemi, Atık Isı Geri Kazanımı, Enerji ve Ekserji Analizi, Eksergoekonomik Analiz, Çevresel Etki, Marib - Yemen.

Bilim Kodu **:** 91436

ACKNOWLEDGMENT

The completion of this thesis would not have been possible without the grace of the Almighty Allah, the Most Merciful and Beneficent, who showered me with His plentiful blessings.

I would like to take this opportunity to extend my deepest appreciation to my supervisor, Assist. Prof. Dr. Abdulrazzak Ahmed Saleh AKROOT, for his immense support, motivation, and guidance in helping me finish this endeavor of mine. I would like to thank him also for helping me learn EES simulation tool.

The completion of this work would not have been possible without the love and support of my family and friends. The names are too numerous to mention but I will keep it short and simple. I would like to thank my family, especially my mother Mrs. Nadya El-Ebbi, and my father Mr. Nabil Al-Arashi for their continuous love and support in this journey of life and in any possible manner when I was far away from my parents. I will forever be indebted for their love, patience and wisdom.

Last but not least, I am grateful to my friends whose presence, support and humor have provided an extra boost for me to complete this journey.

CONTENTS

Page

Page

LIST OF FIGURES

Page

LIST OF TABLES

Page

SYMBOLS AND ABBREVITIONS INDEX

SYMBOLS

c : exergy cost per unit ($/GJ)

COP : coefficient of performance

$\dot{C}$: cost Rate ($/hr)

$\dot{E}$: exergy (kW)

f : exergoeconomic factor (%)

h : specific enthalpy (kJ/kg)

$\dot{m}$: mass flow rate (kg/s)

P : pressure (kPa)

$\dot{Q}$: heat transfer (kW)

s : specific entropy (kJ/kg. K)

T : temperature (°C)

$\dot{W}$: work done (kW)

Z : initial cost rate ($/hr)

ŋ : thermal efficiency (%)

τ : operation hour (h)

φ *:* maintenance factor

ψ : exergy efficiency (%)

ABBREVITIONS

Abs : absorber

CC : Combustion chamber

CCHP : Combined cooling, heating, and power

Comp : compressor

Cond : condenser

EV : expansion valve

Evap : Evaporator

GT : Gas turbine

Gen : generator

HRVG : Heat recovery vapor generation

ARC : absorption refrigeration cycle

HE : heat exchanger

HRSG : heat recovery steam generation

HTF : heat transfer fluid

ORC : organic Rankine cycle

ORT : organic Rankine turbine

P : pump

PART 1

INTRODUCTION

1.1. INTRODUCTION TO INNOVATIVE CCHP SYSTEMS

As traditional power sources are increasingly used, energy security and environmental implications are vital concerns. Combined cooling, heating, and power (CCHP) systems efficiently generate power, heat, and cooling from one fuel source. These systems use waste heat from power generation to meet cooling and heating needs, reducing energy consumption and greenhouse gas emissions. This integration reduces operating carbon footprint and increases energy efficiency, meeting global sustainability targets [1].

Traditional combined heat and power systems use fossil fuels like natural gas, with environmental and financial risks. However, adding solar, biomass, or geothermal power to CCHP technology is changing the paradigm. Advanced fuel cells and microturbines are used in modern combined heat and power systems to reduce fossil fuel use and boost energy efficiency. Improved CCHP (combined heating and cooling) technology allows energy independence in homes, businesses, and industries and promotes sustainability [2].

Cogeneration, or CCHP, has quietly increased power plant efficiency for decades. CCHP systems employ power-generation waste heat. Captured heat can heat a facility, saving energy. This procedure goes beyond heating. CCHP trigeneration powers absorption refrigeration using waste heat. They provide air conditioning, electricity, heat, and chilled water. The versatility of trigeneration benefits industrial buildings, hospitals, and organizations with varying energy needs. CCHP systems are more enticing when integrated with solar or biomass energy. This minimizes fossil fuel use and pollution, improving energy future [3].

The high efficiency of CCHP systems changes the energy landscape. They outperform standard power generation systems that squander energy as heat with over 80% operational efficiency. This advantage is significant as global energy demands rise. CCHP systems dramatically cut energy usage by capturing and using waste heat, reducing carbon emissions. Furthermore, CCHP systems improve energy security and reliability. CCHP creates power on-site and supplies it to consumers, unlike grid-based systems. This removes long-distance energy transmission and distribution losses. Localized power generation gives more control and independence, enabling a more stable energy supply, especially in grid-disrupted areas [4].

CCHP systems have benefits but also drawbacks. Complex equipment might increase upfront costs. These systems need careful site-specific design and operation to work well. Unlike traditional systems, CCHP must be customized to meet each location's energy needs. Despite these obstacles, technology is enabling wider adoption. Due to new materials and control methods, CCHP designs are becoming cheaper and more efficient. An increasing focus on sustainable energy solutions is also pushing CCHP forward. Trigeneration can help meet energy targets, say policymakers, engineers, and environmentalists. CCHP's efficiency, sustainability, and climate change resilience provide a cleaner, more secure energy future [5].

1.1.1. CCHP Systems Work

CCHP systems are more efficient than traditional power generation, which wastes heat. They create power, heating, and cooling from one fuel source. The heat loss of conventional methods is eliminated. The brilliance of CCHP is turning trash into a resource. The heat from power generation, usually lost, drives the system. CCHP converts waste heat into power using an organic Rankine cycle (ORC). In addition, an absorption refrigeration cycle (ARC) uses collected heat to cool water. This clever integration increases energy production efficiency, lowers operational costs, and reduces environmental effects [3].

CCHP system requires a gas turbine or engine to generate electricity. This process generates much heat, which would otherwise be lost to the atmosphere. Heat recovery

devices recuperate this wasted thermal energy in CCHP systems. This recovered energy efficiently heats facilities or drives absorption refrigeration systems for cooling. CCHP systems enhance energy efficiency and reduce operational costs and environmental effects by integrating power, heat, and cooling [6].

In addition to efficiency, CCHP systems improve environmental sustainability. CCHP systems reduce fuel usage and greenhouse gas emissions by eliminating separate heating and cooling systems. CCHP systems' ability to combine renewable energy sources like biomass or solar thermal energy boosts their environmental friendliness. This versatility, combined with large energy savings and decreased carbon footprint, makes CCHP a key technology for more sustainable and resilient energy infrastructures, especially in a world with strict climate goals [6].

1.1.2. Advantages of CCHP Systems

CCHP systems have several characteristics that make them appealing for energy management in industrial and residential settings. The key advantages [3,7,8]:

- CCHP systems use power-generated waste heat for heating and cooling, improving energy efficiency. This integrated technique can reach 80% or more efficiency than individual systems that waste energy.
- CCHP systems reduce fossil fuel use and greenhouse gas emissions by efficiently using fuel to produce multiple energy outputs. This helps battle global climate change.
- Over time, CCHP systems reduce energy expenditures by improving efficiency. Generators that create power, heat, and cooling reduce the cost of buying them separately.
- CCHP systems produce electricity, heat, and cooling locally, enhancing energy reliability. Hospitals and data centers must reduce grid failures and electricity dependence.
- CCHP systems generate energy on-site and reduce grid dependence, promoting energy security. This is significant in countries with unpredictable energy supplies or energy independence goals.

- CCHP systems reduce fossil fuel use and greenhouse gas emissions by efficiently using fuel to produce multiple energy outputs. This helps battle global climate change.
- Customizable CCHP systems fit site energy needs. Flexible, they can be sized to fit the structure or facility.
- CCHP systems save energy costs and increase efficiency, making businesses and institutions more competitive and boosting local economies.
- CCHP systems can be tailored to site energy needs. They're adaptable because they can be sized to fit the building.

1.1.3. Applications of CCHP Systems

CCHP systems can be used anywhere energy, heating, and cooling are needed. Some major CCHP applications are [9–11]:

- Many industrial processes demand plenty of electricity, heat, and cooling. Chemical, pharmaceutical, and manufacturing sectors can reduce energy costs and improve process efficiency with CCHP systems.
- District energy applications benefit from CCHP systems' ability to service many buildings or communities from a central energy plant. Urban areas benefit from this energy distribution optimization.
- Data centers need stable electricity and cooling to run computers and prevent data loss. CCHP systems can power modern data centers without disruptions and meet their massive cooling needs.
- Dormitory, laboratory, and classroom energy needs vary on large university campuses. Energy system students can learn from CCHP systems' sustainable solutions to these diverse needs.
- Hospitals and Healthcare Facilities need regular power, heating, and cooling for patient safety and medical equipment operation. CCHP systems are more resilient to power outages since they supply reliable and emergency power.
- CCHP systems cut energy costs and increase energy efficiency in office buildings, hotels, and large retail complexes. On-site energy generation minimizes peak energy loads and utility dependence.

- CCHP systems can provide heat, electricity for lighting, and cooling in greenhouses to ensure optimal growing conditions year-round.

CCHP systems improve energy efficiency, cost savings, environmental impact, and energy security for these applications, making them essential to sustainable and resilient energy planning.

1.2. BRAYTON CYCLE

Gas turbines operate on the thermodynamic Brayton cycle, named after George Brayton, who developed it in 1872. The Brayton Cycle uses air and fuel to generate work that can power several vehicles by giving them thrust. Compression, combustion, and expansion of flowing air to create work and power compression are the essential phases in extracting energy. Since it powers aircraft, helicopters, and submarines, the Brayton Cycle is very valuable [12–14].

The gas turbine engine compresses air and ignites the fuel in a combustion chamber to power the Brayton cycle. High-energy exhaust gas from combustion turns turbine blades and spinning generator shafts to produce energy. This method shows the cycle's thermal solid efficiency. Reciprocating engines have lower thermal efficiency than the Brayton cycle, which may turn heat energy into work or electricity [15,16].

Brayton cycle fuel adaptability is a significant benefit. This type of gas turbine can run on diesel, biofuels, hydrogen, or natural gas. The Brayton cycle is suited to many industries and power generation demands due to its adaptability [17,18].

The Brayton cycle is used in refrigeration and air conditioning to cool rooms rather than generate power. This adaption shows the Brayton cycle's adaptability and efficiency, which have made it a staple of modern energy systems. The Brayton cycle's efficiency in energy transfer and conversion makes it vital to energy technology progress. The Brayton cycle is essential to satisfying modern energy needs as technology advances and clean energy sources become more important. Its extensive

application and adaptability ensure it adapts to shifting energy environments and provides important solutions [15].

Forthmore, the Brayton cycle is crucial to modern power generation and a thermodynamic invention. Its efficiency, fuel flexibility, and application versatility make it essential in the energy sector. As the world moves toward more sustainable energy, the Brayton cycle's capacity to integrate with renewable energy sources and increase performance and environmental impacts ensure its continued importance [17]..

1.3. ORGANIC RANKIN CYCLE

The Brayton cycle is crucial to modern energy production, although it uses fossil fuels, posing sustainability and environmental concerns. Climate change and fossil fuel depletion drive global interest in renewable energy sources like the Organic Rankine Cycle (ORC). ORCs generate energy using organic fluids like refrigerants or hydrocarbons instead of fossil fuels, making them more sustainable than the Brayton cycle [19,20].

The ORC operates like the Brayton cycle but with adjustments for renewable energy sources like solar and geothermal. The heat from renewable sources vaporizes an organic working fluid in ORCs, propelling a turbine to generate mechanical work and energy. ORCs are ideal for waste heat recovery in industry and transportation because they can use lower-temperature heat sources [21].

Due to organic fluids ' lower boiling points, ORCs can operate at lower temperatures and pressures. Traditional Brayton cycle setups cannot recover energy from various heat sources. This adaption does. However, ORC performance and efficiency depend strongly on the working fluid, and these systems are complicated and require precise design and maintenance, which can increase initial costs and operational demands [22].

Despite these problems, ORCs are being used in more applications due to the need for sustainable and efficient energy. Beyond power generation, ORCs are used in waste heat recovery and combined heat and power systems to reduce energy waste and improve efficiency. This topic needs more research and development since these applications have compelling environmental and economic benefits [23].

The Organic Rankine Cycle has drawbacks, but its benefits make it a sustainable power generation option. To maximize efficiency and application, ORC technology must progress in material science and system integration. Support from governments, businesses, and research institutions can help overcome constraints and unlock ORCs' full potential in the global energy environment, enabling a more sustainable and efficient future [24].

1.4. THE SYNERGY OF GAS TURBINES AND ORC IN CCHP

Gas turbines paired with Organic Rankine Cycle (ORC) systems in combined heat and power (CCHP) applications can improve energy efficiency and sustainability in commercial and industrial environments. Although gas turbines can generate power, their high-temperature exhaust gasses are generally squandered. Organic Rankine Cycle (ORC) systems convert waste heat into electricity, increasing energy efficiency [25].

Integrating gas turbines with ORC systems increases their efficiency, making them better for reliable electricity delivery. Organic fluids with low boiling points are used in the Organic Rankine Cycle (ORC) to convert gas turbine exhaust heat into thermal energy efficiently. The heat generated drives a secondary turbine, generating extra power without fuel. With global initiatives to promote greener energy generation, this technology maximizes fuel utilization and minimizes operational costs and carbon emissions [26].

CCHP systems with ORC technology recover energy more efficiently. After the gas turbine and ORC generate energy, an absorption chiller can heat or cool the surplus heat. CCHP systems' tri-generation technology reduces energy waste in hospitals,

universities, and large commercial buildings, which need constant heating, cooling, and power [27].

Gas turbine-based CCHP systems using Organic Rankine Cycle (ORC) technology increase energy-generating diversity. System settings prioritize electricity, heating, and cooling output based on energy needs and budget. To maximize energy efficiency and operational stability, an energy supply must be able to adapt to shifting load needs and seasonal changes [28].

Gas turbine-ORC CCHP systems are a significant improvement over earlier energy management method. These technologies improve the energy sector's environmental responsibility, cost-effectiveness, and energy efficiency by reusing trash. Growing demand for sustainable energy solutions will drive the usage of integrated CCHP systems with gas turbines and ORC. This idea could improve power generation [29].

1.5. ABSORPTION REFRIGERATION CYCLE

Absorption refrigeration cycle (ARC) is distinct from mechanical refrigeration systems. The heat absorption system uses lithium bromide and water as refrigerants. This method uses thermal energy instead of mechanical energy. Water separates as vapor in the generator when lithium bromide and water are heated under pressure. The vapor cools in the condenser and condenses into liquid, releasing heat and lowering the ambient temperature [30,31].

As liquid water enters the evaporator, it rapidly evaporates and expands. The temperature drops further as this phase transition absorbs heat from the environment. The vaporized water returns to the absorber to recombine with diluted lithium bromide and water, generating heat and completing the cycle. This cyclical mechanism lets ARC cool continuously by transferring heat [30]..

Energy efficiency is a significant benefit of absorption refrigeration systems. ARS uses less electricity by using heat from industrial waste or renewable energy like solar or geothermal power. This reduces operating costs and promotes sustainable energy

consumption, making ARS an environmentally friendly alternative for many applications [32].

ARS' more straightforward mechanical design with fewer moving parts than compression refrigeration systems improve its durability and reliability. Simple systems require less maintenance and last longer, saving money over time. The system is also suited for large-scale applications in hospitals, hotels, and food processing factories where reliable and efficient cooling is needed [32].

ARS has several benefits, but it costs more to install and performs poorly at higher temperatures than standard systems. Environmental benefits like lower greenhouse gas emissions and non-ozone-depleting refrigerants justify their wider adoption. Absorption refrigeration systems will play a more significant part in sustainable cooling solutions as technology progresses and more cost-effective solutions are produced, emphasizing the need for continuing innovation and support [33].

1.6. THESIS OBJECTIVE

The achieved objectives of thermodynamic, exergoeconomic, and environmental analysis of the CCHP system are summarized as follows:

- To evaluate CCHP energy efficiency. The system's energy flow and transformations are examined to see how well it converts input energy into electricity, heating, and cooling.
- To assess CCHP system cost-effectiveness using exergy analysis and economic concepts. This includes calculating the system's energy efficiency improvements' genuine economic worth and the most economically possible configuration.
- To evaluate the decrease in the CCHP system's greenhouse gas (GHG) emissions compared to traditional systems. This will assist in determining how CCHP systems can support sustainable development.

1.7. OUTLINE OF THE THESIS

The first chapter provides an overview of the innovative CCHP Systems, encompassing introductory information on the Brayton cycle, organic Rankine cycle, the synergy of gas turbines and ORC in CCHP, and the absorption refrigeration cycle. Chapter Two thoroughly explores the literature on new CCHP Systems. In the third chapter of this thesis, the model's main components and mechanisms are explained. The third chapter also covers the CCHP system's input parameters and thermodynamic, exergoeconomic, and environmental equations used in its energy, exergy, economic, and environmental analysis. The study results and discussion are in the fourth chapter. Chapter 5 summarizes this work.

PART 2

LITERATURE REVIEW

CCHP systems represent a technological advancement in sustainable energy solutions, particularly when incorporating renewable energy sources as heat sources. The growing interest from researchers in these technologies is evident through various theoretical and experimental studies, reflecting their potential benefits for industrialization. The relevant literature is summarized as follows:

Huang et al. [34] examined a SOFC-GT hybrid power cycle CCHP system extensively. They performed multi-objective optimization to balance thermodynamic efficiency, economic costs, and environmental implications. The results enhanced performance metrics and achieved 65.15% system exergy efficiency under equal target weighting. The system was 78.55% energy, 65.73% electrical, and 61.20% exergy efficient. The optimized system cut CO2 to 0.2742 kg/kWh. Economics and the environment benefited from 3.43% and 8.84% cost and CO2 emission reductions, respectively. The study highlighted the system's efficient, eco-friendly cooling, heating, and energy production. The study showed hybrid systems can improve efficiency and emissions with careful design and control optimization.

Du and Guo [35] introduced a novel CCHP system that integrates various cycles and technologies to improve thermodynamic, economic, and environmental performance, especially under low load. Waste heat utilization and load regulation are enhanced by the proposed CCHP system's unique combination of the GTC, ORC, supercritical CO2 Brayton recompression cycle (SCRC), ARC, and compressed air energy storage (CAES). The system's thermodynamic performance increased, lowering unit energy costs and greenhouse gas emissions, especially at low loads. Economic research shows the CCHP system's 2.44-year payback period proving cost-effectiveness. The environmental assessment shows lower greenhouse gas equivalent emissions,

supporting sustainable energy. The study finds the CCHP system promising for energy efficiency and environmental conservation. The CCHP system improves thermodynamic, economic, and ecological performance, especially at low loads. The system decreases greenhouse gas emissions to 0.313 kgCO2e/kWh2 and has 75.99% energy and 45.89% exergy efficiency at the lowest load. The planned CCHP system has a 2.44-year payback, making it cost-effective. According to the study, advanced CAES approaches improve CCHP system operational flexibility, which is essential for handling different load requirements.

Lucarelli et al. [36] presented a CCHP system merging GTC, SCRC, ORC, and Absorption ARC with CAES. Thermodynamic performance was improved by compressor bypass extraction for variable load regulation. CCHP systems have a 2.44-year payback period and minimize greenhouse gas emissions, especially during low-load operations. CAES helps store and reuse bypass removed air, enhancing system efficiency and stability. Their findings stressed the need to choose industry-specific technology and techniques to boost efficiency and reduce environmental impact.

Wang et al. [37] assessed a new CCHP system using WHR from a regenerative BC's techno-economic and environmental impacts. A multi-objective optimization minimizes costs, ecological consequences, and technological efficiency. The system had an optimal energy efficiency of 77.17%, exergetic efficiency of 38.94%, levelized total yearly emissions of 9.36 kg/kW.yr, and expenses of 106.04 €/kW.yr. CCHP has a 3.74-year payback period and a net present value of 1,184,525.43 €, confirming economic feasibility. The study introduced Levelized Total Annual Emissions (LTAE) to assess the system's environmental efficiency based on annual energy production. The innovative CCHP system design improved energy efficiency, fuel consumption, and pollutant emissions, promoting sustainable energy development. The results showed that waste heat recovery can improve CCHP system performance and sustainability, solving industrial energy waste.

Datacenter CCHP system optimization was studied by Norani et al. [38]. The study compares two operational scenarios to provide an optimal energy supply architecture for a data center CCHP system. The second scenario uses absorption chiller refrigerant

to cool the Organic Rankine Cycle (ORC) condenser, improving cooling capacity, energy efficiency, and exergy efficiency. The exergoeconomic analysis shows that the second operating scenario has a lower overall fuel and product cost rate in the CCHP system. The best energy supply design reduces primary energy use, saving energy and the environment. The energetic and exergetic evaluations show that the second scenario improves CCHP system performance. Compared to the first scenario, cooling capacity, energy efficiency, and exergy efficiency increase by 30.66%, 14.18%, and 13.48%. According to the exergoeconomic analysis, the second scenario reduces fuel and product-related costs by 38.9% and 31.58%, making it more economically viable. Liu et al. [39] performed an exergoeconomic analysis and multi-objective optimization of a SOFC/GT-integrated CCHP system with transcritical CO2 power and refrigeration cycle. Their work optimized system performance using advanced simulation methods to balance energy efficiency and economic factors. Using CO2's natural refrigerant qualities, transcritical CO2 cycles can reduce CCHP systems' carbon footprint and improve environmental sustainability. CCHP, which combines SOFC/GT with transcritical CO2 power/refrigeration cycles, has many advantages over standard energy systems.CCHP systems use waste heat for heating and cooling, increasing primary energy efficiency. Some studies show that gas-powered CCHP systems can lower pollutant emissions by 40%. CCHP systems save a lot of primary energy. A combined system that recovers and uses waste heat can save 23.1% more energy than typical systems. They work with renewable energy sources and are ideal for household and industrial use. CCHP systems are more sustainable and environmentally friendly than conventional energy systems, which are less efficient and emit more.

Nond and Gogo [40] discussed a CCHP system that generates chilled water, process heat, and power. This system had an inter-cooled-recuperative GTC, ARC, and HRSG. Using low-grade heat from air compression intercooling and flue gas to drive the absorption cooling system and heat recovery steam generator is the major innovation. System performance was assessed using energy, exergy, exergoeconomic, and environmental studies. It produced 30 MW of electricity, 29.92 MW of process heat, and 4.72 MW of cooling with 83.79% energy and 50.60% exergy efficiency. The

results revealed a 2.53% exergy efficiency increase, 13.62% system cost reduction, and 18.67% environmental cost reduction.

Jia et al. [41] studied a unique CCHP system with biomass gasification, SOFC, a micro gas turbine (MGT), and an absorption chiller. Their rigorous 3E (energy, exergy, and economic) evaluation showed how biomass might be used as a renewable energy source in CCHP systems to minimize fossil fuel use and increase sustainability. The results showed that biomass moisture content, gasifier air flow rate, and fuel gas temperature significantly affect energy and exergy performance. Higher airflow and lower biomass moisture content boost CCHP output and efficiency. Boost gasifier airflow to boost exergy efficiency by 10%. Biomass with moisture below 0.2 has exergy efficiency above 45% and CCHP efficiency over 65%. Lowering exhaust gas temperature to 90°C increases CCHP system efficiency by 10%. Electrical, exergy and CCHP efficiency can exceed 50%, 40%, and 80%, respectively. Economically, SOFC's initial investment is 50%-60% of CCHP's total investment and pays back in 7-8 years.

Lei et al. [42] studied a CCHP system using an MGT-powered ORC. They extensively analyzed energy and exergy to determine system synergies and thermodynamic losses. The authors used a parametric analysis to examine how ORC evaporating temperature, turbine efficiency, and absorption refrigeration chiller-producing temperature affect system performance. They tested six organic working fluids to assess system impact: R141b, Toluene, D4, n-octane, n-heptane, and MM. The system's primary energy efficiency and exergy efficiency may reach 76.89% and 54.95% with toluene as the working fluid. ORCs as middle cycles improve CCHP system efficiency and reduce exergy destruction. Their studies showed that absorption chillers improve CCHP system efficiency and environmental performance by utilizing waste heat.

Chahartaghi et al. [43] studied a CCHP system using a steam turbine (ST) to save energy and waste. This study analyzed and optimized the system's performance to find the most significant energy efficiency, economic viability, and environmental effect trade-offs. According to their research, STs can improve CCHP system operational flexibility and efficiency, especially in industrial environments with significant power

and heat demands. Compared to typical systems, the CCHP system reduced operational expenses by 35.34%, fuel usage by 15.83%, and carbon dioxide emissions by 24.91%. ST inlet temperatures and pressures affect system performance. The study found an 82.46% tri-generation efficiency, improving system performance.

Zeng et al. [44] investigated a SOFC-CCHP system with a supercritical CO2 power cycle, ORC, and ARC. This study demonstrated the thermodynamic efficiency of high-efficiency power cycles to maximize energy use and decrease losses. Integrating these distinct cycles increased operational range and system efficiency using waste heat at different temperatures. The simulation showed that the system had a net power efficiency of 59.62%, an overall energy efficiency of 77.61%, an exergy efficiency of 59.08%, and a SOFC-generated electrical efficiency of 43.18%. System exergy losses are 383.29 kW and 372.46 kW, respectively, according to conventional and graphical exergy analysis, with a 2.91% relative error. Both analysis methodologies show that the SOFC component destroys over 65% of system exergy.

Hai et al. [45] studied a town's CCHP energy, cooling, and heating system. The system includes a GT for topping cycle electricity generation, an ORC, and a DEACH for bottoming cycle cooling. This setup uses GT waste energy to generate electricity, cooling, and heating. The study used thermodynamic modeling and energy, exergy, and economic assessments. Exergy-based sustainability analyses evaluate environmental implications. The study used parametric analysis to assess how design characteristics affect operational results and multi-objective optimization to balance exergy efficiency and Total Cost Rate. The optimization's optimum point showed an exergy efficiency of 17.56%, a TCR of $74.49 per hour, and a sustainability index of 1.21, demonstrating the system's ability to use waste heat from small-scale GTs to meet town-level energy needs.

Wang et al. [46] developed a sustainable fossil fuel alternative CCHP system using solar thermochemical (STC) processes and TES. Solar energy powers a methane steam reforming (MSR) reaction that produces hydrogen-rich syngas to generate electricity for a high-efficiency SOFC and MGT arrangement. A double-effect lithium bromide unit cools, and a HE heats WHR from this procedure. A parabolic trough collector

(PTC) boosts heating and cooling. Simulations of adaptability to weather and user expectations allow the system to satisfy hourly requests exactly. It had high summer, transitional, and winter total exergy efficiencies of 69.93%, 62.03%, and 52.28%, respectively, with CO2 emissions of 152.57, 191.75, and 234.16 g/kWh. These numbers showed the system's efficiency and environmental benefits, especially under extreme sun radiation. Economic research showed a $779.34k original cost and ninth-year profitability, a major step toward sustainable energy solutions.

García-Domínguez et al. [47] extensively studied the thermodynamic performance of a zero-emission solar-powered trigeneration system using computational methods based on the first and second laws of thermodynamics and an exergy-based methodology. A PTC-heated ORC is used. A cascade single-effect H2O/LiBr absorption heat pump is connected to this ORC. The optimized system had 152.4% energy efficiency, 21.1% exergy efficiency, and 17.5% electrical-exergy efficiency. It generated 82.1 kW, 200.4 kW, and 471.7 kW of power, cooling, and heating. SPTCs account for 73% of exergy loss, according to the report. Additionally, the solar field outlet temperature and ORC condensation temperature greatly affect system performance.

Musharavati et al. [48] studied a geothermal-based CCHP system with a thermoelectric generator (TEG) using thermodynamic modeling, exergo-economic analysis, and multi-objective optimization. The CCHP/TEG system was simulated using the Engineering Equation Solver (EES), and an exergo-economic model was created to assess energy stream costs. Parametric research using thermodynamic and economic criteria found 139.7 kW of net production power and 807 kW of total useable products. The system had 55.81% energy and 22.63% exergy efficiency. Multi-objective optimization employed the ideal point approach to establish optimal operating conditions to maximize exergy efficiency and minimize electricity cost rate. This adjustment yielded $12.52 per hour in electrical costs and 22.11% exergy efficiency. It also found ideal turbine inlet pressure and separation temperature at 8 and 13 bars, respectively.

Nazari et al.[49] proposed solar pre-heating for a biomass-based CCHP system with an externally fired GT, ORC, and absorption chiller. This system used solar thermal energy for pre-heating to maximize waste heat usage and efficiency. Thermal and economic analyses showed that the system had first- and second-law efficiencies of 55.56% and 20.38%, respectively, and significantly higher power, heating, and cooling outputs than typical configurations. Exergy and exergo-economic analysis identified key losses and inefficiencies. A new optimization technique improved the system's exergy efficiency to 22.20% and reduced its cost to $24.86 per hour, showing superior performance in multi-objective optimization settings.

Asgari et al. [50] evaluated a trigeneration system with a GT, MSW gasification, and LiBr-Water absorption refrigeration cycle using a baseline design with a 50% MSW mixing ratio. According to the study, summer performance was 30 units of net power output, increased fuel consumption, and lower cooling efficiency. This caused seasonal differences in Energy Utilization Factors (EUF) and exergy efficiency. The system produced reliable electricity, heat, and cooling with a consistent MSW flow rate throughout the year, although the gasification unit and heat exchangers caused significant exergy losses.

Wang et al. [51] developed a sophisticated trigeneration system with a GTC, regenerative sCO2 Brayton cycle, ORC, and ARC. The GTC waste heat was efficiently channeled into the sCO2 cycle, then the ORC for power generation, and the ARC for cooling. GTC intercoolers provide hot water. Comprehensive thermodynamic and exergoeconomic analyses evaluated the ORC's performance with various working fluids and optimized the system. The improved system produced 40.65 MW of power, 6.02 MW of cooling, and 9.93 MW of heating with a 20.17% exergoeconomic factor. The GTC has the most considerable exergy destruction and capital expenses, followed by the sCO2 cycle, ORC, and ARC. System performance depended on working fluid, affecting unit costs and exergy efficiencies but decreasing thermal efficiencies. The most expensive combustion chamber affected the system's economic and thermodynamic performance, especially during optimization.

Abd El-Sattar et al. [52] modeled a trigeneration system that uses sugarcane bagasse from Qena and Aswan, Upper Egypt, to generate power, cooling, and heat. Direct biomass burning was done in a combustion chamber at atmospheric pressure coupled to an externally fired gas turbine (EFGT), ORC, and ARC. Cyclohexane, benzene, toluene, and R113 were tested as ORC working fluids to determine the best one based on the heat source-to-boiling point temperature difference. Simulations showed that toluene was the best working fluid for CCHP applications. The system's performance parameters include 177.56 kW of net electric power generation, 142.92 kW from the EFGT, and 34.64 kW from the ORC, totaling 24.2% net electrical efficiency, 38.50 kW cooling capacity, and 43.50% CCHP efficiency. The system was tuned for 144 kg/h biomass consumption.

Zare and Takleh[53] designed a geothermal-driven CCHP system that combines an ejector transcritical CO2 cycle with a Rankine cycle. They suggested replacing the gas cooler with an internal heat exchanger (system b) to boost system efficiency. These arrangements' first and second-law performances were assessed using thermodynamic models, and design variables were examined using parametric analysis. Replacing the gas cooler with an internal heat exchanger increased the system's exergy efficiency, net output power, and cooling output by 30.9%, 49.1%, and 75.8%. This change reduces heating output by 39.1%. The study also noted that enhanced thermodynamic cycles and geothermal energy may boost CCHP system efficiency and performance.
Parikhani et al. [54] created a modified Kalina cycle CCHP system that uses a Low-temperature heat source (LTHS) to power an ammonia-water mixture. The study assessed system viability using thermodynamic and thermoeconomic methods. The system has 49.83% energy efficiency, 27.68% exergy efficiency, and $198.3 per GJ unit product cost. With a 32.03% exergy destruction ratio, Condenser 2 caused system irreversibility. The study found that increasing the evaporation temperature and basic ammonia (NH3) concentration or reducing the separator pressures, heating unit temperature, and vapor generator Terminal Temperature Difference (TTD) improved energy efficiency. The cycle's total cost could peak with evaporation temperature variations. Adjusting Separator 1 pressure and elemental ammonia concentration could improve it. The research concluded that careful operational parameter adjustment

could significantly impact this revolutionary CCHP system's performance and cost-efficiency.

Zhang et al. [55] introduced a CCHP system with a sCO2 power cycle, tCO2 power cycle, and DH system. The tCO2 cycle generates power and drives a CO2-based refrigeration cycle using waste heat from the sCO2 cycle, making this system unique. The DH system also heats using waste heat from the sCO2 and tCO2 cycles and the refrigeration compressor outflow. The study found that the CCHP system could increase exergy efficiency by 12.01% and reduce total product unit cost by 5.14%, or at least 10.83% and 4.12%, compared to a standalone sCO2 power cycle. These findings showed that the CCHP system has considerable thermodynamic and economic benefits across demand scenarios.

Saini et al. [56] developed a solar-powered, compact, and sustainable CCHP system for distant tiny structures. Evacuated tube collectors, TES, an ORC, an ejector refrigeration cycle, and a water heater provided electricity, cooling, and heating in this system. System performance was measured by exergy efficiency, cooling cost, heating cost, power cost, total cost per total output, and equivalent carbon dioxide emissions. Parametric studies examined how generator, evaporator, condenser, pinch point temperature difference, and turbine mass fraction affected system performance. The system has 3.159% exergy efficiency, a $2023 annual cost, and 13.10 tons of CO2 emissions. Adjustments in generator or evaporator temperature increased exergy efficiency and CO2 emissions but raised heating costs and lowered cooling and power expenses. Hotter condensers lowered exergy efficiency and cooling/power costs but increased heating and CO2 emissions. Additionally, increasing turbine mass fraction improved exergy efficiency and power costs but decreased cooling costs and the cooling-power cost ratio. Since it balances economic, environmental, and efficiency factors, the CCHP system suits remote slight building cooling, heating, and electricity needs.

Razmi et al. [57] developed a cogeneration system using CCHP, CAES, an ORC, and a hybrid compression-absorption refrigeration cycle. The developed system used of residual heat from turbine exhaust gases for cooling via an ORC-driven refrigeration

system to increase CAES system efficiency. The design examined how the maximum and minimum pressure ratio affects CAES vessel volume and round-trip efficiency (RTE). It used compression-absorption refrigeration and high-temperature thermal energy storage (HTES) with R407C as the organic working fluid to reduce fossil fuel use and improve environmental sustainability. The performance showed that the system can generate 2280 kW of electricity and 416.7 kW of cooling at peak hours. The RTE enhanced from 13.15% to 65.15% over a solo CAES system. The system destroyed 1419 kW of exergy and had a 49.17% efficiency. Potential efficiency improvements were found in the pressure regulating valve and air turbine, which had the highest irreversibility and exergy destruction. This system advanced building energy efficiency and sustainability.

Rostamzadeh et al. [4] developed two innovative micro-combined (micro-CCHP) systems that integrate either an ORC or a Kalina Cycle (KC) as topping cycles, coupled with an ejector refrigeration cycle (ERC) and a vapor compression heat pump cycle (VCHPC) as bottoming cycles. The feasibility of these systems was evaluated using detailed thermodynamic modeling and exergoeconomic analysis. The results indicated that the KC-based micro-CCHP system achieves higher optimum thermal efficiency and a higher total sum unit cost of the product (SUCP) than the ORC-based system. However, it has a lower exergy efficiency. Specifically, the thermal efficiencies measured were 77.32% for the KC system and 76.54% for the ORC system, while the exergy efficiencies were 31.2% for KC and 48.37% for ORC. The generator was pinpointed as the primary source of exergy destruction in both configurations.

Zhang et al. [58] developed a biomass-geothermal CCHP system with biomass gasification, CAES, a biogas turbine for power generation, and a ground source heat pump. The CAES was powered by off-peak electricity and stored high-pressure air ignited with biomass gasification biogas. Absorption chillers and GSHPs use waste heat to cool and heat. According to the study, the system has 90.06% round trip efficiency and 31.52% exergy efficiency. A dynamic payback period of 3.032 years is projected for the $908,008 system equipment capital investment. The research also found that increasing the HE air outlet temperature boosts energy and exergy

efficiency. These efficiencies vary with gas turbine inlet temperature and air storage cavern inlet and outflow pressures.

Moghimi et al. [59] investigated a novel configuration of a CCHP system that integrates a BC, an RC, an ERC, and a domestic water heater, employing a comprehensive 4E (energy, exergy, economic, and environmental) analysis framework. The study commenced with an evaluation of performance using energy and exergy analyses, complemented by an environmental assessment to understand the impacts relative to a traditional Brayton cycle. The findings revealed that the CCHP system demonstrates enhanced exergy and energy efficiencies over the conventional BC. Key design variables, including the GTIT, compressor pressure ratio, HRSG pressures, HRSG pinch point temperatures, and regenerator effectiveness, were found to affect the system's performance significantly. The research concluded that the CCHP system improves exergy efficiency by 7% and boosts energy efficiency by 12% compared to the Brayton cycle, underscoring its enhanced performance and potential environmental advantages.

Mehrpooya et al. [60] introduced a novel concentrated solar power system with a desalination process and absorption refrigeration cycle, providing power, fresh water, and refrigeration. This revolutionary system uses parabolic dish collectors to create 21,030 kW of thermal energy to drive a steam turbine that generates 4,632 kW of electricity. A single-stage ammonia-water absorption refrigeration system produces 820.8 kW, and a multi-effect desalination process produces 22.79 kg/s of fresh water. Analysis indicated that the distillation column and heat exchangers destroy 86% of system exergy. The system has 66.05% exergy and 80.70% net thermal efficiency. The system is expected to have a 5.738-year investment payback and a $6.828 million net yearly profit. A sensitivity analysis shows the system's strong economic and operational sustainability by determining how different factors affect performance.

Eisavi et al. [61] developed a solar-powered CCHP system using an ORC, a double-effect lithium bromide-waterARC, and HEs to generate electricity, cooling, and heating. Even though it reduces electrical production, a double-effect refrigeration system in solar-driven CCHP systems improves thermal efficiency, according to the

study. The system was thoroughly examined for energy and exergy efficiency to identify losses. The study found that replacing a single-effect absorption chiller with a double-effect system in CCHP configuration boosts cooling power by 48.5%, enhancing system performance. This adjustment also increases heating power by 20.5%, increasing cogeneration heat and power efficiency to 96.0%. Net electrical power generation drops 27% with this arrangement. The study also found a significant exergy degradation rate in solar collectors, suggesting this is an area for efficiency improvements.

Moghimi et al. [62] studied a sophisticated CCHP system with a thermal vapor compression multi-effect desalination system that produced power, fresh water, refrigeration, and hot water for home use. A dual-pressure heat recovery steam generator unit links the Brayton cycle to water desalination and ejector refrigeration in this multipurpose system. The study found that the system efficiently supplies 85.57 kg/s, 30 MW, 2.03 MW, and 1.11 MW of fresh water, power, cooling, and heating. Total exergy destruction was 55.82 MW, with 36.03% exergy efficiency and 39.22% energy efficiency. These findings show that the system can efficiently meet different energy and water needs, but exergy and energy efficiencies can be improved to improve performance and reduce environmental impact.

PART 3

SOLUTION METHODOLOGY

3.1. SYSTEM DESCRIPTION

CCHP systems integrate multiple energy technologies, including the Brayton cycle, organic Rankine cycle (ORC), and absorption refrigeration, to produce electricity, heat, and cooling, as seen in Figure 3.1. In these systems, fuel is burned in a gas turbine or another combustion engine to power an electric generator. The waste heat generated in this process is then harnessed to supply heating and cooling by utilizing the ORC cycle and absorption refrigeration techniques.

The Brayton cycle is a thermodynamic process utilized in gas turbines to convert fuel into energy. Within this cycle, the air is initially compressed by an air compressor, heated in a combustion chamber by burning the fuel, and expanded in a turbine to generate work. After this expansion, the air is discharged into the Heat Recovery Vapor Generator (HRVG) in the current model to use as a heat source for the ORC model.

The ORC model is a thermodynamic cycle that employs an organic fluid having a lower boiling point than water instead of water. This makes it ideal for turning low-grade heat into electricity. The cycle begins with liquid organic working fluid. The fluid is pushed via an HRVG that absorbs BC's exhaust heat. The fluid vaporizes into a high-pressure gas when heated. In a turbine, high-pressure vapor expands and cools. This expansion powers a turbine and generator to generate energy. Vapor enters a condenser after the turbine. Releases heat to the environment and condenses back into liquid. A feed pump raises the liquid's pressure to finish the cycle. Power is generated by repeating this procedure. Toluene was chosen as the working fluid for the ORC in this research because of its exceptional thermal stability, which allows it to endure

high temperatures and severe thermal stress. This substance's excellent boiling point and advantageous physical features enable effective heat transfer from waste heat sources. Moreover, the non-corrosive properties of toluene mitigate the potential for equipment deterioration and decrease maintenance expenses. Toluene's extensive availability and cost-effectiveness make it a realistic option for converting industrial waste heat into power.

The lithium bromide absorption refrigeration cycle is a specific kind of absorption refrigeration system that mainly utilizes water and lithium bromide as the absorbent. This cycle is prevalent in applications such as air conditioning systems, where heat is the primary energy source instead of electricity. The cycle starts in the evaporator, where low-pressure water (refrigerant) assimilates thermal energy from the surrounding environment (such as air or water that requires cooling). The heat leads the water to undergo evaporation, resulting in the removal of heat and the generation of a cooling effect. A concentrated lithium bromide solution in the absorber then absorbs the water vapor generated in the evaporator. The absorption process is exothermic, meaning it releases heat. A cooling water circuit often eliminates this heat. The lithium bromide solution undergoes water vapor absorption, resulting in the formation of a diluted solution. Subsequently, the lithium bromide solution, which has been diluted, is pressurized and directed towards the generator. Heat is introduced to the generator's high-pressure, diluted lithium bromide solution, usually by hot water or steam. Applying heat induces water evaporation from the solution, resulting in the restoration of concentrated lithium bromide and the liberation of water vapor. The generator in the current model uses the heat of the exhaust gases. The water vapor produced in the generator is then condensed into liquid form in the condenser, releasing its latent heat. The condensed water is then returned to the evaporator to begin the cycle. The residual lithium bromide solution remaining in the generator after desorption is cooled, if required, and then returns to the absorber to undergo the absorption process again.

In the current model, the generator utilizes the heat from the exhaust gases discharged from the HRVG as its heat source. Additionally, a portion of the cooling load generated by the Absorption Refrigeration Cycle (ARC) is used to cool the atmospheric air before it enters the Brayton Cycle (BC) model.

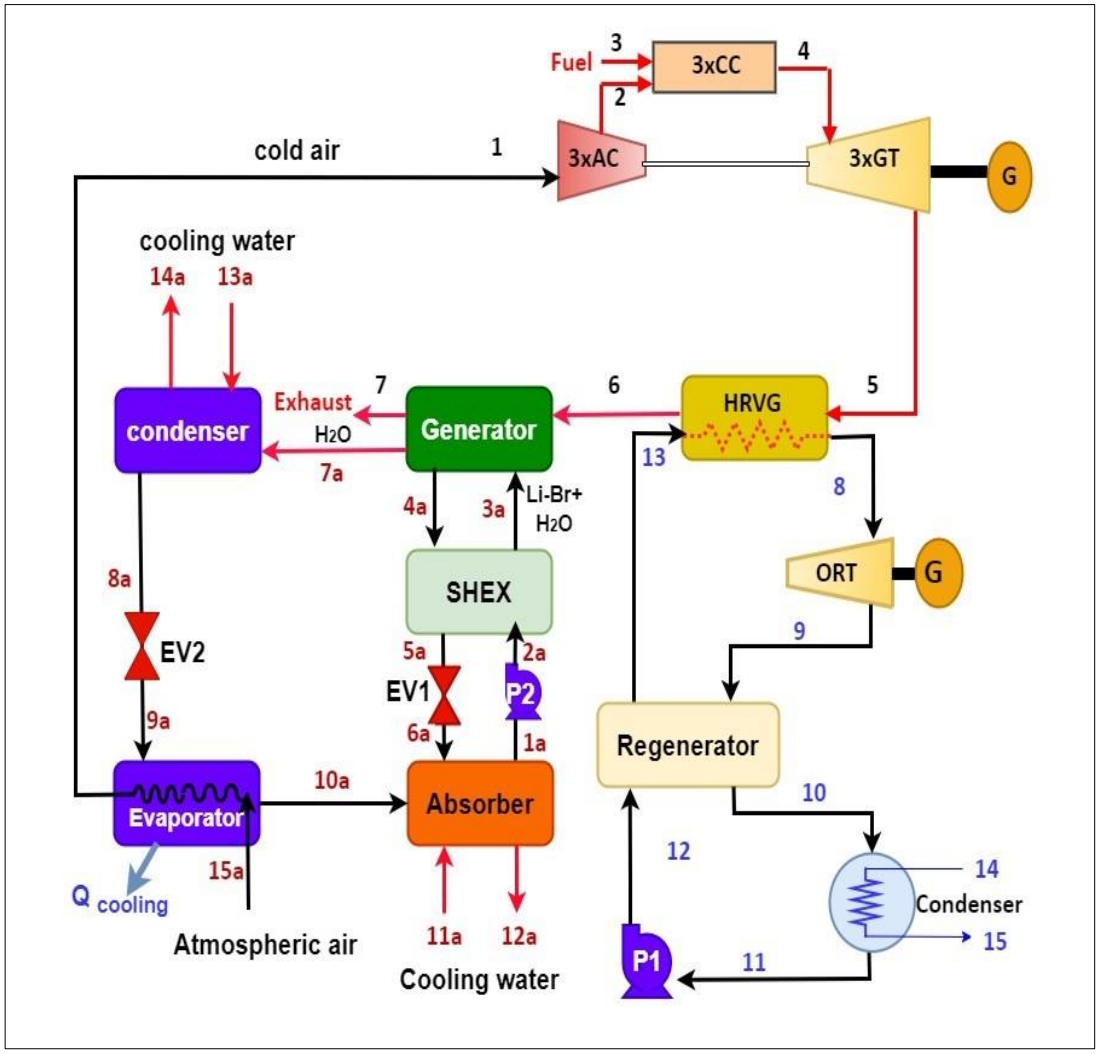

Figure 3.1. Schematic Diagram of the CCHP system.

The thermodynamic analysis of the trigeneration cycle incorporates several assumptions, as outlined below:

- All processes within the cycle are assumed to be in a steady-state condition.
- The analysis utilizes the control volume method.
- The fuel entering the combustion chamber is natural gas, specifically 100% methane, with a lower heating value (LHV) of 50,056 kJ/kg.
- Pressure losses in the refrigeration cycle, including those in heat exchangers and pipelines, are considered negligible.
- Saturated vapor is used as the working fluid entering the steam turbine.
- The refrigerant (water) exiting the evaporator is assumed to be in a saturated vapor state.

- The refrigerant (water) exiting the condenser is assumed to be a saturated liquid.
- The temperature of the refrigerant vapor leaving the generator is estimated as the average temperature of the inlet and outlet solutions.
- Lithium bromide (LiBr) solutions in the generator and absorber are assumed to be in equilibrium with their respective temperatures and pressures.

3.2. ENERGY ANALYSIS OF THE CCHP SYSTEM

The principles of continuity and the first law of thermodynamics are summarized as follows [63–65]:

$$\sum \dot{m}_{in} = \sum \dot{m}_{out} \tag{3.1}$$

$$\sum (\dot{m}h)_{in} - \sum (\dot{m}h)_{out} + \left(\sum \dot{Q}_{in} - \sum \dot{Q}_{out}\right) + \dot{W} = 0 \tag{3.2}$$

The mass balance equation for Li/Br is stated as follows:

$$\sum [\dot{m}x]_i - \sum [\dot{m}x]_o = 0 \tag{3.3}$$

where:

$\dot{m}$ the mass flow rate.
$\dot{Q}$ the heat input.
$\dot{W}$ the work produced.
h the enthalpy.

And the terms 'in' and 'out' in the subscript refer to the inlet and outlet states, respectively.

The equations derived from performing an energy balance on the components of the Brayton Cycle (BC) are presented as follows:

Air compressor:

$$\dot{m}_1 = \dot{m}_2 \tag{3.4}$$

$$\dot{W}_{AC} = \dot{m}_1(h_2 - h_1) \tag{3.5}$$

Combustion chamber:

$$\dot{m}_2 + \dot{m}_3 = \dot{m}_4 \tag{3.5}$$

$$\dot{m}_2 h_2 + \eta_{CC}\dot{m}_3 \text{LHV} = \dot{m}_4 h_4 \tag{3.6}$$

Gas turbine:

$$\dot{m}_4 = \dot{m}_5 \tag{3.7}$$

$$\dot{W}_{GT} = \dot{m}_4(h_4 - h_5) \tag{3.8}$$

Where η_{CC} and LHV are the efficiency of the CC and the lower heating value of the fuel.

The equations derived from performing an energy balance on the components of the ORC are presented as follows:

HRVG Model:

$$\dot{m}_5 + \dot{m}_{13} = \dot{m}_6 + \dot{m}_8 \tag{3.9}$$

$$\dot{m}_5 h_5 + \dot{m}_{13} h_{13} = \dot{m}_6 h_6 + \dot{m}_8 h_8 \tag{3.10}$$

Organic Rankine turbine:

$$\dot{m}_8 = \dot{m}_9 \tag{3.11}$$

$$\dot{W}_{ORT} = \dot{m}_8(h_8 - h_9) \tag{3.12}$$

Regenerator Model:

$$\dot{m}_9 + \dot{m}_{12} = \dot{m}_{10} + \dot{m}_{13} \tag{3.13}$$

$$\dot{m}_9 h_9 + \dot{m}_{12} h_{12} = \dot{m}_{10} h_{10} + \dot{m}_{13} h_{13} \tag{3.14}$$

Condenser Model:

$$\dot{m}_{10} = \dot{m}_{11} \tag{3.15}$$

$$\dot{m}_{14} = \dot{m}_{15} \tag{3.16}$$

$$\dot{Q}_{con} = \dot{m}_{10}(h_{10} - h_{11}) \tag{3.17}$$

Organic Rankine Pump:

$$\dot{m}_{11} = \dot{m}_{12} \tag{3.18}$$

$$\dot{W}_{ORP} = \dot{m}_{11}(h_{12} - h_{11}) \tag{3.19}$$

The equations resulting from the energy balance analysis of the ARC components are outlined below:

Generator (Gen):

$$\dot{m}_{3a} = \dot{m}_{4a} + \dot{m}_{7a} \tag{3.20}$$

$$\dot{m}_{3a} x_{3a} = \dot{m}_{4a} x_{4a} \tag{3.21}$$

$$\dot{Q}_{gen} = \dot{m}_{4a}h_{4a} + \dot{m}_{7a}h_{7a} - \dot{m}_{3a}h_{3a} = \dot{m}_{6}(h_{6} - h_{7}) \quad (3.22)$$

Condenser (Con2):

$$\dot{m}_{7a} = \dot{m}_{8a} \quad (3.23)$$

$$\dot{m}_{13a} = \dot{m}_{14a} \quad (3.24)$$

$$\dot{Q}_{con2} = \dot{m}_{7a}(h_{7a} - h_{8a}) \quad (3.25)$$

Evaporate (Evap):

$$\dot{m}_{9a} = \dot{m}_{10a} \quad (3.26)$$

$$\dot{Q}_{Evap} = \dot{m}_{9a}(h_{10a} - h_{9a}) \quad (3.27)$$

Absorber (ABS):

$$\dot{m}_{10a} + \dot{m}_{6a} = \dot{m}_{1a} \quad (3.28)$$

$$\dot{m}_{6a}x_{6a} = \dot{m}_{1a}x_{1a} \quad (3.29)$$

$$\dot{Q}_{ABS} = \dot{m}_{10a}h_{10a} + \dot{m}_{6a}h_{6a} - \dot{m}_{1a}h_{1a} \quad (3.30)$$

Solution heat exchange (SHE):

$$\dot{m}_{4a}h_{4a} + \dot{m}_{2a}h_{3a} = \dot{m}_{3a}h_{3a} + \dot{m}_{5a}h_{5a} \quad (3.31)$$

$$\dot{m}_{4a} + \dot{m}_{2a} = \dot{m}_{3a} + \dot{m}_{5a} \quad (3.32)$$

Pump:

$$\dot{m}_{1a} = \dot{m}_{2a} \tag{3.33}$$

$$\dot{W}_P = \dot{m}_{1a}(h_{2a} - h_{1a}) \tag{3.34}$$

The first law (energy) efficiency of the Combined Cooling, Heating, and Power (CCHP) cycle is defined as the ratio of the useful output energy to the input energy of the system:

$$\eta_{\text{CCHP}} = \left(\dot{W}_{net} + \dot{Q}_{cooling}\right)/\dot{Q}_{CC} \tag{3.35}$$

$$\dot{W}_{net} = \dot{W}_{GT} - \dot{W}_{AC} + \dot{W}_{ORT} - \dot{W}_{ORP} - \dot{W}_P \tag{3.36}$$

$$\dot{Q}_{cooling} = \dot{Q}_{Evap} - \dot{m}_{1}(h_{15a} - h_1) \tag{3.37}$$

$\dot{Q}_{cooling}$ is the produced rate of cooling load.

$$\dot{Q}_{CC} = \eta_{CC}\dot{m}_3 \text{LHV} \tag{3.38}$$

3.3. EXERGY ANALYSIS OF THE CCHP SYSTEM

The common approach to evaluating a physical or chemical process involves formulating an energy balance using the first law of thermodynamics. However, this law focuses solely on the quantity of energy, neglecting its quality. Exergy analysis addresses this limitation by considering both the quantity and the quality of energy.
The exergy rate represents the maximum theoretical useful work achievable as the system transitions from its initial state to a state of thermal and mechanical equilibrium with the surrounding environment. This rate is expressed by the following formula [66]:

$$\dot{\text{E}}_i = \dot{m}_{\text{i}}(h_i - h_0) - T_0(s_i - s_o) \tag{3.39}$$

The exergy balance for a system in steady state is defined in the following way[67]:

$$\dot{\mathrm{E}}_f = \dot{\mathrm{E}}_p + \dot{\mathrm{E}}_{dis} \tag{3.40}$$

Where $\dot{\mathrm{E}}_f$, $\dot{\mathrm{E}}_p$, and $\dot{\mathrm{E}}_{dis}$ are the exergy flow of fuel, exergy flow of product, and exergy destruction. In the context of second law analysis, the rate of exergy destruction is equivalent to the loss of potential to convert energy into useful work. The exergy efficiency of a system is assessed by evaluating the fuel and product exergy of the component based on the concept of surplus efficiency in exergy terms [68]:

$$\Psi = \frac{\dot{\mathrm{E}}\mathrm{x}_p}{\dot{\mathrm{E}}\mathrm{x}_f} = 1 - \frac{\dot{\mathrm{E}}\mathrm{x}_{des}}{\dot{\mathrm{E}}\mathrm{x}_f} \tag{3.41}$$

Ψ is exergy efficiency. The equations derived from performing an exergy balance on the components of the CCHP system are presented as follows:

Air compressor:

$$\dot{E}_{D,AC} = \dot{W}_{AC} - \left(\dot{E}_2 - \dot{E}_1\right) \tag{3.42}$$

$$\psi_{\mathrm{AC}} = 1 - \frac{\dot{E}_{D,AC}}{\dot{W}_{AC}} \tag{3.43}$$

Combustion chamber:

$$\dot{E}_{D,CC} = \dot{E}_2 + \dot{E}_3 - \dot{E}_4 \tag{3.44}$$

$$\psi_{CC} = 1 - \frac{\dot{E}_{D,CC}}{\dot{E}_2 + \dot{E}_3} \tag{3.45}$$

Gas turbine:

$$\dot{E}_{D,GT} = \left(\dot{E}_4 - \dot{E}_5\right) - \dot{W}_{GT} \tag{3.46}$$

$$\psi_{GT} = 1 - \frac{\dot{E}_{D,GT}}{\dot{E}_4 - \dot{E}_5} \tag{3.47}$$

HRVG:

$$\dot{E}_{D,HRVG} = \left(\dot{E}_5 + \dot{E}_6\right) - \left(\dot{E}_8 + \dot{E}_{13}\right) \tag{3.48}$$

$$\psi_{HRVG} = 1 - \frac{\dot{E}_{D,HRVG}}{\dot{E}_5 + \dot{E}_6} \tag{3.49}$$

Organic Rankine turbine:

$$\dot{E}_{D,ORT} = \left(\dot{E}_8 - \dot{E}_9\right) - \dot{W}_{ORT} \tag{3.50}$$

$$\psi_{ORT} = 1 - \frac{\dot{E}_{D,ORT}}{\dot{E}_8 - \dot{E}_9} \tag{3.51}$$

Recuperator:

$$\dot{E}_{D,Rec} = \left(\dot{E}_9 + \dot{E}_{10}\right) - \left(\dot{E}_{13} + \dot{E}_{12}\right) \tag{3.52}$$

$$\psi_{Rec} = 1 - \frac{\dot{E}_{D,Rec}}{\dot{E}_9 + \dot{E}_{10}} \tag{3.53}$$

Condenser:

$$\dot{E}_{D,cond} = \left(\dot{E}_{10} + \dot{E}_{11}\right) - \left(\dot{E}_{15} + \dot{E}_{14}\right) \tag{3.54}$$

$$\psi_{cond} = 1 - \frac{\dot{E}_{D,cond}}{\dot{E}_{10} + \dot{E}_{11}} \tag{3.55}$$

Organic Rankine Pump:

$$\dot{E}_{D,ORP} = \dot{W}_{ORP} - \left(\dot{E}_{12} - \dot{E}_{11}\right) \tag{3.56}$$

$$\psi_{ORP} = 1 - \frac{\dot{E}_{D,ORP}}{\dot{W}_{ORP}} \tag{3.57}$$

Generator:

$$\dot{E}_{D,Gen} = \left(\dot{E}_{6} - \dot{E}_{7}\right) - \left(\dot{E}_{4a} - \dot{E}_{3a} + \dot{E}_{7a}\right) \tag{3.58}$$

$$\psi_{Gen} = 1 - \frac{\dot{E}_{D,Gen}}{\dot{E}_{6} - \dot{E}_{7}} \tag{3.59}$$

Condenser 2:

$$\dot{E}_{D,Con2} = \left(\dot{E}_{7a} - \dot{E}_{8a}\right) - \left(\dot{E}_{14a} - \dot{E}_{13a}\right) \tag{3.60}$$

$$\psi_{Gen} = 1 - \frac{\dot{E}_{D,Con2}}{\dot{E}_{7a} - \dot{E}_{8a}} \tag{3.61}$$

Evaporator:

$$\dot{E}_{D,Evap} = \left(\dot{E}_{15a} - \dot{E}_{1}\right) + \dot{E}Q_{cooling} - \left(\dot{E}_{10a} - \dot{E}_{9a}\right) \tag{3.62}$$

$$\psi_{Evap} = 1 - \frac{\dot{E}_{D,Evap}}{\left(\dot{E}_{1a} - \dot{E}_{1}\right) + \dot{E}Q_{cooling}} \tag{3.63}$$

Absorber:

$$\dot{E}_{D,ABS} = \left(\dot{E}_{10a} - \dot{E}_{1a} + \dot{E}_{6a}\right) - \left(\dot{E}_{11a} - \dot{E}_{12a}\right) \tag{3.64}$$

$$\psi_{ABS} = 1 - \frac{\dot{E}_{D,ABS}}{\left(\dot{E}_{10a} - \dot{E}_{1a} + \dot{E}_{6a}\right)} \tag{3.65}$$

SHEX:

$$\dot{E}_{D,SHEX} = \left(\dot{E}_{4a} - \dot{E}_{5a}\right) - \left(\dot{E}_{3a} - \dot{E}_{2a}\right) \tag{3.66}$$

$$\psi_{SHEX} = 1 - \frac{\dot{E}_{D,SHEX}}{\left(\dot{E}_{4a} - \dot{E}_{5a}\right)} \tag{3.67}$$

Pump:

$$\dot{E}_{D,P} = \dot{W}_P - \left(\dot{E}_{2a} - \dot{E}_{1a}\right) \tag{3.68}$$

$$\psi_P = 1 - \frac{\dot{E}_{D,P}}{\dot{W}_P} \tag{3.69}$$

The second law (exergy) efficiency of the CCHP cycle is defined as the ratio of the useful output energy to the input exergy of the system:

$$\psi_{\mathrm{CCHP}} = \left(\dot{W}_{net} + \dot{E}Q_{cooling}\right)/\dot{E}_3 \tag{3.70}$$

$$\dot{E}Q_{cooling} = \left(1 - \frac{\mathrm{T}_o}{T_{Evap}}\right)\dot{Q}_{cooling} \tag{3.71}$$

3.4. EXERGOECONOMIC ANALYSIS OF THE CCHP SYSTEM

Exergoeconomic analysis is an effective method that integrates thermodynamic principles (exergy) and economic theory to evaluate energy systems. This approach not only focuses on energy efficiency but also examines the economic worth of the energy utilized [69]. This section integrates exergy and economic concepts . Table 3.1 lists the main constant parameters used for calculations. The costs of purchased equipment ($\dot{Z}_k$ and CRF), which are utilized in the exergoeconomic evaluation, are detailed in Table 3.2.

Table 3.1. Constant parameters used in exergoeconomic analysis for calculating investment costs.

Parameter	Symbol	Value
Interest rate (%)	i	10
Working hours in a year	N	8000
Number of a lifetime year	n	25
Maintenance factor	φ	1.06

The investment cost rate and cost recovery factor are calculated using the following formulas [70,71]:

$$\dot{Z}_k = \frac{Z_k \times CRF \times \phi}{N \times 3600} \tag{3.72}$$

$$\mathrm{CRF} = \frac{i(1+i)^n}{(1+i)^n - 1} \tag{3.73}$$

The costs of purchased equipment ($\dot{Z}_k$), which are utilized in the exergoeconomic evaluation, are detailed in Table 3.2.

Table 3.2. Functions for Purchased Equipment Cost ($\dot{Z}_k$) used in exergoeconomic evaluations [14,72].

Component	Cost function
AC	$z_{AC} = 71.1x\left(\frac{\dot{m}_{air}}{0.9-\eta_{comp}}\right) \times r_p \times \ln(r_p)$
CC	$z_{CC} = 46.08 \times \frac{\dot{m}_a}{0.995-\frac{P_4}{P_2}} \times \left(1 + \exp(0.018 \times T_4 - 26.4)\right)$
GT	$z_{GT} = 479.34 \times \frac{\dot{m}_5}{0.93-\eta_{GT}} \times \ln\left(\frac{P_4}{P_5}\right) \times \left(1 + \exp(0.036 \times T_4 - 54.4)\right)$
HRVG	$z_{HRVG} = 235 \times \dot{Q}^{0.75}$
ORT	$z_{ORT} = 479.34 \times \frac{\dot{m}_8}{0.93-\eta_{ORT}} \times \ln\left(\frac{P_8}{P_9}\right) \times \left(1 + \exp(0.036 \times T_8 - 54.4)\right)$
Con	$z_{Con} = 1773 \times \dot{m}_{10}$
ORP	$z_{ORP} = 2100 \times \left(\frac{W_{ORP}}{10}\right)^{0.26} \times \left(\frac{1-\eta_{\mathrm{ORP}}}{\eta_{\mathrm{ORP}}}\right)^{0.5}$
Reg	$z_{\mathrm{Re}g} = 235 \times \dot{Q}^{0.75}$
ABS	$z_{ABA} = 16000(\mathrm{A}_{ABS}/100)^{0.6}$
ABS	$z_{SHEX} = 309.14(\mathrm{A}_{\mathrm{SHEX}})^{0.85}$
Pump	$z_{\mathrm{P}} = 17585(\mathrm{W}_{\mathrm{P}}/100)^{0.71}\left(1 + \frac{0.2}{1-\eta_{\mathrm{P}}}\right)$
Gen	$z_{Gen} = 17500(\mathrm{A}_{\mathrm{Gen}}/100)^{0.6}$
Evap	$z_{Evap} = 16000\left(\mathrm{A}_{\mathrm{Evap}}/100\right)^{0.6}$
Exp. valve	$z_{\mathrm{E}xp.valve} = 114.5\dot{\mathrm{m}}_{\mathrm{water}}$

The exergoeconomic balance for each component encompasses the cost rate of exergy flows and investment-related expenses [73]:

$$\sum \dot{C}_{in,k} + \dot{Z}_k = \sum \dot{C}_{out,k} \tag{3.74}$$

The average cost per unit of exergy for fuel and product, along with the cost of exergy destruction—which is determined by the extent of exergy destruction and the unit cost of fuel exergy—are calculated as follows:

$$c_{F,k} = \frac{\dot{C}_{F,k}}{\dot{E}_{F,k}} \tag{3.75}$$

$$c_{P,k} = \frac{\dot{C}_{P,k}}{\dot{E}_{P,k}} \tag{3.76}$$

$$\dot{C}_{D,k} = c_{F,k}\dot{E}_{D,k} \tag{3.77}$$

The exergoeconomic factor, which are dimensionless coefficients, indicate the economic performance of the equipment as follows:

$$f_k = \frac{\dot{Z}_k}{\dot{Z}_k + \dot{C}_{D,k}} \tag{3.78}$$

The overall investment cost can be determined using the equation below [74]:

$$\dot{C}_{system} = \sum \dot{Z}_k + \sum \dot{C}_{D,k} + \dot{C}_F + \dot{C}_{env} \tag{3.79}$$

The rate of cost associated with fuel entering the combustion chamber is [73]:

$$\dot{C}_F = c_f \times \dot{m}_f \times LHV \tag{3.80}$$

Where $c_f$is the unit cost of fuel (methane gas), c_f, is 12 \$/GJ. The rate of the cost associated with the environment is calculated as follows [74] :

$$\dot{C}_{env} = c_{CO_2} \times \dot{m}_{CO_2} \tag{3.81}$$

Where c_{CO_2} is the unit cost of CO_2, c_{CO_2} is 0.024 \$/kJ. The total cost of electricity per unit of energy, expressed in dollars per megajoule (\$/MJ), is derived using the formula below:

$$\dot{C}_{electricity} = \frac{\dot{C}_{system}}{\dot{W}_{net}} \tag{3.82}$$

Table 3.3. Presents the cost balances and auxiliary equations for each component of the system.

Component	Exergetic cost rate balance equation	Auxiliary Equation
AC	$\dot{C}_1 + \dot{C}_{W,AC} + \dot{Z}_{AC} = \dot{C}_2$	$c_{w,AC} = c_{w,GT}$
CC	$\dot{C}_2 + \dot{C}_3 + \dot{Z}_{CC} = \dot{C}_4$	$\frac{\dot{C}_2}{\dot{E}_2} = \frac{\dot{C}_4}{\dot{E}_4}$, $c_3 = 12$
GT	$\dot{C}_4 + \dot{Z}_{W,GT} = \dot{C}_5 + \dot{C}_{GT}$	$\frac{\dot{C}_4}{\dot{E}_4} = \frac{\dot{C}_5}{\dot{E}_5}$
HRVG	$\dot{C}_5 + \dot{C}_{13} + \dot{Z}_{HRVG} = \dot{C}_6 + \dot{C}_8$	$\frac{\dot{C}_5}{\dot{E}_5} = \frac{\dot{C}_6}{\dot{E}_6}$
ORT	$\dot{C}_8 + \dot{Z}_{ORT} = \dot{C}_9 + \dot{C}_{ORT}$	$\frac{\dot{C}_8}{\dot{E}_8} = \frac{\dot{C}_9}{\dot{E}_9}$
Reg	$\dot{C}_9 + \dot{C}_{12} + \dot{Z}_{Reg} = \dot{C}_{10} + \dot{C}_{13}$	$\frac{\dot{C}_9}{\dot{E}_9} = \frac{\dot{C}_{10}}{\dot{E}_{10}}$
Con	$\dot{C}_{10} + \dot{C}_{14} + \dot{Z}_{con} = \dot{C}_{11} + \dot{C}_{15}$	$\frac{\dot{C}_{10}}{\dot{E}_{10}} = \frac{\dot{C}_{11}}{\dot{E}_{11}}$
ORP	$\dot{C}_{11} + \dot{C}_{W,ORP} + \dot{Z}_{ORP} = \dot{C}_{12}$	$c_{w,ORP} = c_{w,ORT}$
Gen	$\dot{C}_6 + \dot{C}_{3,a} + \dot{Z}_{Gen} = \dot{C}_7 + \dot{C}_{7,a} + \dot{C}_{4,a}$	$\frac{\dot{C}_{4,a} - \dot{C}_{3,a}}{\dot{E}_{4,a} - \dot{E}_{3,a}} = \frac{\dot{C}_{7,a} - \dot{C}_{3,a}}{\dot{E}_{7,a} - \dot{E}_{3,a}}$
Pump	$\dot{C}_{1,a} + \dot{C}_{W,P} + \dot{Z}_P = \dot{C}_{2,a}$	$c_{w,P3} = c_{w,ORT}$
SHEX	$\dot{C}_{2,a} + \dot{C}_{4,a} + \dot{Z}_{SHEX} = \dot{C}_{3,a} + \dot{C}_{5,a}$	$\frac{\dot{C}_{4,a}}{\dot{E}_{4,a}} = \frac{\dot{C}_{5,a}}{\dot{E}_{5,a}}$
EV1	$\dot{C}_{5,a} + \dot{Z}_{EV1} = \dot{C}_{6,a}$	
ABS	$\dot{C}_{6,a} + \dot{C}_{10,a} + \dot{C}_{11,a} + \dot{Z}_{Abs} = \dot{C}_{1,a} + \dot{C}_{12,a}$	$\frac{\dot{C}_{6,a} + \dot{C}_{10,a}}{\dot{E}_{6,a} + \dot{E}_{10,a}} = \frac{\dot{C}_{1,a}}{\dot{E}_{1,a}}$, $c_{11,a} = 0$
Evaporator	$\dot{C}_{9,a} + \dot{C}_{1,a} + \dot{Z}_{Evap} = \dot{C}_1 + \dot{C}_{10,a}$	$\frac{\dot{C}_{9,a}}{\dot{E}_{9,a}} = \frac{\dot{C}_{10,a}}{\dot{E}_{10,a}}$, $c_{1,a} = 0$
EV2	$\dot{C}_{8,a} + \dot{Z}_{EV2} = \dot{C}_{9,a}$	
Con2	$\dot{C}_{7,a} + \dot{C}_{13,a} + \dot{Z}_{con2} = \dot{C}_{8,a} + \dot{C}_{14,a}$	$\frac{\dot{C}_{7,a}}{\dot{E}_{7,a}} = \frac{\dot{C}_{8,a}}{\dot{E}_{8,a}}$, $c_{13,a} = 0$

3.5. ENVIRONMENTAL ANALYSIS OF THE CCHP SYSTEM

The CO_2 emission rate quantifies the volume of CO_2 that is discharged into the atmosphere as a result of human activities. In the context of power plant operation, the term "intensity" refers to the ratio of total CO_2 emissions produced during a certain time to the total energy generated during the same period. The rate is computed using the following formula equation [75,76]

$$\epsilon_{CO_2} = \frac{\dot{m}_{CO_2}}{\dot{W}_{net}} \tag{3.83}$$

The mass flow rate of CO_2 is calculated using equation (3.84) [63]:

$$\dot{m}_{CO_2} = y_{CO_2} \dot{m}_{g,5} \left(\frac{\bar{M}_{CO_2}}{\bar{M}_g} \right) \tag{3.84}$$

where $\dot{m}_{CO_2}$ and $\bar{M}_{CO_2}$ are the molecular weight and mole fraction of CO_2, respectively. Also, $\dot{m}_g$ and $\bar{M}_g$ are the molecular weight and mole fraction of the exhaust gases at the end of the combustion chamber.

PART 4

RESULTS AND DISCUSSIONS

This chapter first investigates the results of the developed hybrid system's energy exergy, exergoeconomic, and environmental analysis. The influence of adding ORC and ARC is addressed on the overall hybrid system performance. Then, the effect of BC's pressure ratio, GTIT, and ORTIT on the hybrid system's energetic, economic, and exergoeconomic aspects have been considered in this study. To validate the simulation code and its results, this study compares the thermal efficiencies, work outputs, and irreversibility values of the various components within the Brayton cycle with those reported in reference [72]. The same input parameters from Table 4.1 are used for both simulations. Table 4.2 demonstrates a satisfactory concordance between the outcomes of the current program and the findings of [72].

Table 4.1. Input values for the system's Brayton cycle are based on the data reported in [72].

Parameter	**Value**
Ambient pressure and temperature	92.18 kPa and 27°C
Compressor pressure ratio	18.9
Mass flow rate of the air	74.1 kg/s
Gas turbine inlet temperature	1444.1 K
Compressor isentropic efficiency	0.86
Gas turbine isentropic efficiency	0.89
Lower heating value of the fuel	46974 kJ/kg

Table 4.2. Comparative Analysis of Current Programming Code Outcomes and the Brayton Cycle in the Examined System[62].

Parameter	**Code**	**Ref** [72]	***Error (%)***
$\dot{W}_{GT}$ **(MW)**	19.52	19.5	0.1
$\dot{m}_{fuel}$ **(kg/s)**	1.271	1.27	0.16
$\dot{E}_{des,AC}$ **(MW)**	2.260	2.261	-0.04
$\dot{E}_{des,CC}$ **(MW)**	13.353	13.355	-0.015
$\dot{E}_{des,GT}$ **(MW)**	8.4	8.393	0.08

The input values for simulating the combined cycle system depicted in Figure 3.1 are detailed in Table 4.3. It's important to highlight that the exhaust gas temperature at point 4 in the BC is so high that the organic Rankine turbine's inlet temperature is set at 600°C. Additionally, a compressor with a pressure ratio of 11 is chosen for operation to reflect actual plant conditions better.

Table 4.3. Input parameters to simulate the combined cycle systems simulation.

Parameter	**Value**
Compressor pressure ratio	11
Ambient temperature (°C)	26.45
Ambient pressure (°C)	101.3
Lower heating value of fuel(kJ/kg)	50056
Inlet air mass flow rate (kg/s)	500
Isentropic efficiency of the compressor (%)	86
Isentropic efficiency of gas turbine	90
Pinch point of HRVG (°C)	15
Outlet temperature of gases from CC (°C)	1097
The pressure of the ORF at the inlet of HRVG (kPa)	2500
Isentropic efficiency of the ORT	80
Outlet temperature of Condenser (°C)	45.8
Outlet temperature of ARC Condenser (°C)	39
Outlet temperature of evaporator (°C)	5
Outlet temperature of generator (°C)	88
Outlet temperature of absorber (°C)	37

The Engineering Equation Solver (EES) software created the system performance simulation. Thermodynamic properties such as temperature, pressure, entropy, enthalpy, and exergy, along with the mass flow rate at each state point, are detailed in Table 4.4.

Table 4.4. Stream properties for each state.

State	Mass (kg/s)	Pressure (kPa)	Temperature (K)	Enthalpy (kJ/kg)	Entropy (KJ/kg.K)	Exergy (MW)
1	500	101.3	280	262.6	5.666	0
2	500	1115	600.5	591.8	5.755	151.3
3	9.434	101.3	288	-4672	11.53	489
4	509.4	1059	1360	201.8	8.081	482.2
5	509.4	107.7	850.6	-421.6	8.179	149.8
6	509.4	104.5	615	-690.3	7.818	67.71
7	509.4	101.3	375	-949.9	7.293	15.24
8	192.2	2500	600	710.4	1.401	60.1
9	192.2	10.21	476.6	516	1.506	16.71
10	192.2	10.21	330	292.1	0.9508	5.495
11	192.2	10.21	318.8	-122.4	-0.3483	0.2346
12	192.2	2500	319.8	-118.7	-0.346	0.8116
13	192.2	2500	433.3	105.2	0.2498	9.712
14	857.9	101.3	299.5	110.3	0.3854	0
15	857.9	101.3	311.5	160.4	0.5497	0.8427
1a	135.1	310	0.8634	81.92	0.238	5.217
2a	135.1	310.2	6.944	81.93	0.238	5.218
3a	135.1	342.9	6.944	151.5	0.451	6.036
4a	115.5	361	6.944	219.6	0.4816	11.98
5a	115.5	333	6.944	167.2	0.3305	11.13
6a	115.5	321.6	0.8634	167.2	0.3306	11.12
7a	19.61	361	6.944	2656	7.506	5.217
8a	19.61	312	6.944	162.7	0.557	0.02622
9a	19.61	278	0.8634	162.7	0.586	-0.1431
10a	19.61	278	0.8634	2510	9.029	-3.454
11a	4582	298	101.3	104.3	0.3651	0.4497
12a	4582	308	101.3	146.1	0.5031	3.593
13a	2924	298	101.3	104.3	0.3651	0.287
14a	2924	308	101.3	146.1	0.5031	2.293

Utilizing the data from Table 4.3 and applying the formulas outlined in Chapter 3, the findings pertaining to energy, exergy, exergoeconomic, and environmental assessments of this research are compiled in Table 4.5. As can be seen, the net output powers of the Bottoming Cycle (BC) and the Organic Rankine Cycle (ORC) are approximately 153 MW and 36.66 MW, respectively, resulting in a combined system net power output of around 189.6 MW. Additionally, the utilization of waste heat recovery from the Heat Recovery Vapor Generator (HRVG) in the Absorption Refrigeration System (ARS) leads to cooling production rates of approximately 35.79 MW. The combined system's calculated exergetic and energetic efficiencies are 38.78% and 40.16%, respectively. In comparison, BC’s energy and exergy efficiencies are lower, at 30.19% and 31.27%. This signifies an enhancement of 8.59 and 8.89

percentage points in the combined system, attributable to the waste heat recovery from BC. The proposed system's overall cost rate is 38553.18 USD/hr. This includes fuel consumption at 52.5%, capital investment at 2.5%, exergy destruction at 38.8%, and environmental costs at 5.8%. The fuel cost rate is the primary factor contributing to the overall cost rate, with the exergy destruction cost rate coming in second. Consequently, the exergoeconomic factor is calculated at 6.07%. The assessment of the unit cost of specific energy for the products reveals that this metric is identical for the combined system and BC a, amounting to 54.52 USD/GJ and 66.62 USD/GJ, respectively.

The findings reveal that the Brayton cycle's environmental carbon footprint stood at 631 kg/MWh, reduced to 485.5 kg/MWh when utilizing a combined cycle. This underscores the substantial decrease in environmental carbon emissions that can be attained through waste heat recovery from the Brayton cycle.

Table 4.5. Output values in the current study.

Calculated Parameters	**CCHP Model**	**BC Model**
Fuel mass flow rate. $\dot{m}_{fuel}$ (kg/s)	9.434	8.99
Toluene mass flow rate, $\dot{m}_{Toluene}$ (kg/s)	192.2	-
CO_2 mass flow rate, $\dot{m}_{CO_2}$ (kg/s)	25.88	24.66
Gas turbine power, $\dot{W}_{GT}$ (MW)	153	140.7
ORT power, $\dot{W}_{ORT}$ (MW)	36.66	-
Net power, $\dot{W}_{net}$ (MW)	189.6	140.7
Thermal efficiency, η_I (%)	38.78	30.19
Exergy efficiency, η_{II} (%)	40.16	31.27
Exergy destruction,$\dot{E}_{D,Total}$ (MW)	391	177.62
Capital investment cost, $\dot{Z}_{Total}$ ($/hr)	965.68	614.85
Exergy destruction cost, $\dot{C}_{D,Total}$ ($/hr)	14951.5	10042
Fuel cost, $\dot{C}_{Fuel}$ ($/hr)	20400	19439
Environmental cost, $\dot{C}_{Env}$ ($/hr)	2236	2131
Total cost, $\dot{C}_{Total}$ ($/hr)	38553.2	32227
Specific energy unit cost ($/GJ)	54.52	63.62
COP for ARC	0.81	-
Cooling Load, $\dot{Q}_{Cooling}$ (MW)	35.79	-
$C0_2$ emission, ε_{CO2} (kg_{CO_2}/MWh)	485.5	631

Table 4.6 details the flow rates of energy and exergy across various components and the exergy efficiency within the system's components, providing an enhanced understanding of the combined cycle system's performance. As seen in this table, the combustion chamber undergoes the most substantial energy loss attributed to chemical reactions, amounting to 158.1 MW (40.4% of the total exergy destruction. Another significant observation is the increased exergy destruction rate in the HRVG, primarily due to the heat transfer between the exhaust gases and the organic Rankine fluid. The pump exhibits the highest exergy efficiency, while the condenser shows the lowest exergy efficiency among the components of the combined cycle.

Table 4.6. Energy and exergy analysis of the current study.

Component	**W OR Q (MW)**	$\dot{E}_{dest}$ **(MW)**	**Ψ (%)**
Air Compressor	164.607	13.3	91.92
Combustion chamber	472.224	158.1	75.31
Gas turbine	317.583	14.81	95.54
Vapor generator	136.883	31.74	61.36
Organic turbine	37.372	6.019	86.13
Regenerator	223.8	2.315	79.36
Condenser	43.034	4.418	16.02
Pump1	0.709	0.1323	81.35
Absorber	57.461	6.281	33.58
Pump2	0.521	0	100
Heat exchanger	9.392	0.03	96.58
Generator	56.985	17.07	39.53
Expansion valve1	0	0.17	84.58
Condenser	48.894	3.185	38.64
Expansion valve2	0	0.003	99.97
Evaporator	46.026	3.025	8.65

Table 4.7 displays the exergoeconomic analysis for each component of the combined cycle. This table highlights that economically, the combustion chamber warrants significant consideration as it has the highest cost factor, $\dot{Z}_K + \dot{C}_D$, totaling 8303 USD/hr. The HRVG, air compressor, and gas turbine rank subsequently in terms of elevated overall cost rates. Moreover, the data presented in this table show that the combustion chamber possesses the minimal exergoeconomic factor among all components. The derived value for this component suggests that the cost associated with exergy destruction outweighs the initial cost, leading to a diminished

exergoeconomic factor. It should also be highlighted that the overall exergoeconomic factors for the combined cycle amount to 6.07 percent. The findings reveal that the cost rate of exergy destruction considerably exceeds that of the initial equipment cost. Consequently, opting for components with a higher upfront cost can enhance the overall system efficiency.

Table 4.7. Exergoeconomic analysis of the current study.

Component	$\dot{C}_D$ **($/h)**	$\dot{Z}_K$ **($/h)**	$\dot{Z}_K + \dot{C}_D$ **($/h)**	**f (%)**
Air Compressor	1010	342.2	1352	25.31
Combustion chamber	8302.88	0.12	8303	0.0023
Gas turbine	1033	272.7	1305	20.9
Vapor generator	2213	24.41	2237	1.091
Organic turbine	724.4	246.6	971	25.4
Regenerator	278.6	0.2	278.8	0.071
Condenser	531.6	4.976	536.6	0.927
Pump1	23.78	0.28	24.06	1.162
Absorber	0.2578	2.8892	3.147	91.81
Pump2	0	0.03466	0.03466	100
Heat exchanger	0.0029	0.4771	0.48	99.4
Generator	0.6963	6.5357	7.232	90.37
Expansion valve1	0.00006	0.03494	0.035	99.83
Condenser	0.02144	0.54116	0.5626	96.16
Expansion valve2	0.00034	0.20566	0.206	99.84
Evaporator	14.33	4.46	18.79	23.74
Total system	14951.5	965.68	15971.2	6.07

Figure 4.1 illustrates how the pressure ratio of the Brayton Cycle (BC) influences several key parameters: the power generated by the BC cycle itself, the power output of the Organic Rankine Cycle (ORC), the total power output of the combined system, and the cooling load of the Absorption Refrigeration Cycle (ARC). It is observed that a rise in the pressure ratio of the BC enhances the power output from the gas turbine (GT) yet negatively affects the power output of the Organic Rankine Cycle (ORC). The underlying reason is that an increase in pressure ratio reduces the gas turbine's exhaust temperature, consequently diminishing the amount of energy available for the ORC cycle to harness. As a result, the ORC's mass flow rate decreases, reducing its power generation. Generally, the decrease in power production by the ORC cycle outweighs the increase in power from the gas turbine, resulting in a net reduction in the overall cycle's power output. Referring to Figure 4.1, it is observed that elevating

the Brayton Cycle's (BC) pressure ratio results in a reduction of the total system's net power output, dropping from 197.2 MW to 162.4 MW.

Conversely, less waste energy is available for recovery in the vapor generator due to the reduction in the organic fluid's mass flow rate. This limitation maintains the input energy level in the absorption refrigeration system's generator. Consequently, the system's cooling capacity stays at 35.9 MW as the total pressure ratio escalates from 6 to 20. It's important to highlight that a portion of the cooling load generated by the ARC is utilized to pre-cool the ambient air before it enters the air compressor.

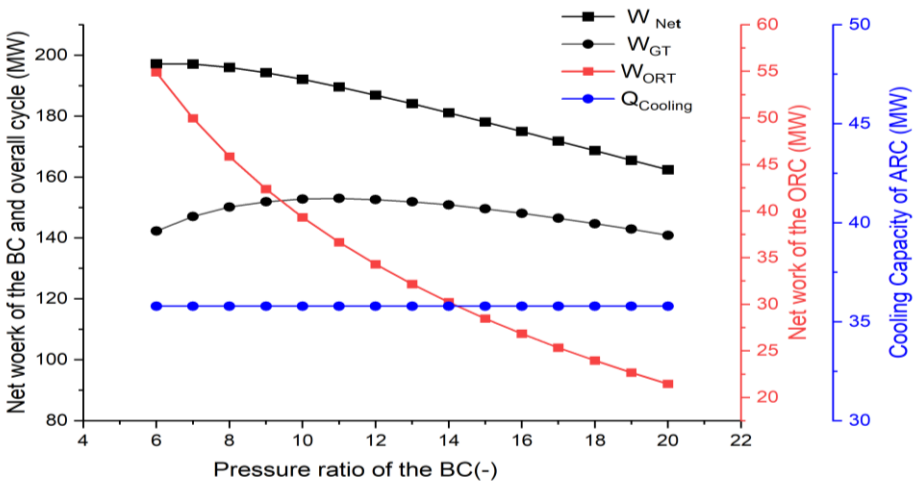

Figure 4.1. Effects of the BC's pressure ratio on the net power output of BC cycle, the net power output of ORC, the net power output of the overall system, and the cooling load of the ARC.

Figure 4.2 depicts the influence of the Brayton Cycle (BC) pressure ratio on the total cost rate, energy cost per unit, and capital investment requirements. The figure indicates that both fuel and environmental costs decrease as the Brayton Cycle (BC) pressure ratio rises. This decrease is attributed to the reduction in fuel consumption and CO2 emissions associated with a higher-pressure ratio, which in turn lowers fuel and environmental costs. As depicted in Figure 4.2, an increase in the pressure ratio of the Brayton Cycle (BC) leads to a decline in fuel expenses, dropping from 22,964 USD/hr to 17,349 USD/hr, and a reduction in environmental costs from 2,515 USD/hr to 1,902 USD/hr. The figure also illustrates that the exergy destruction cost decreases as the Brayton Cycle's (BC) pressure ratio rises, but the capital investment cost

increases. The cost per unit of energy first decreases, reaching a low point, before it begins to climb again with further increases in the BC's pressure ratio. This pattern is linked to the decrease in power output from the overall cycle at higher pressure ratios, which in turn raises the cost per unit of energy. It is noted that the lowest specific energy cost, at 54.03 $/GJ, occurs at a pressure ratio of 14 bar.

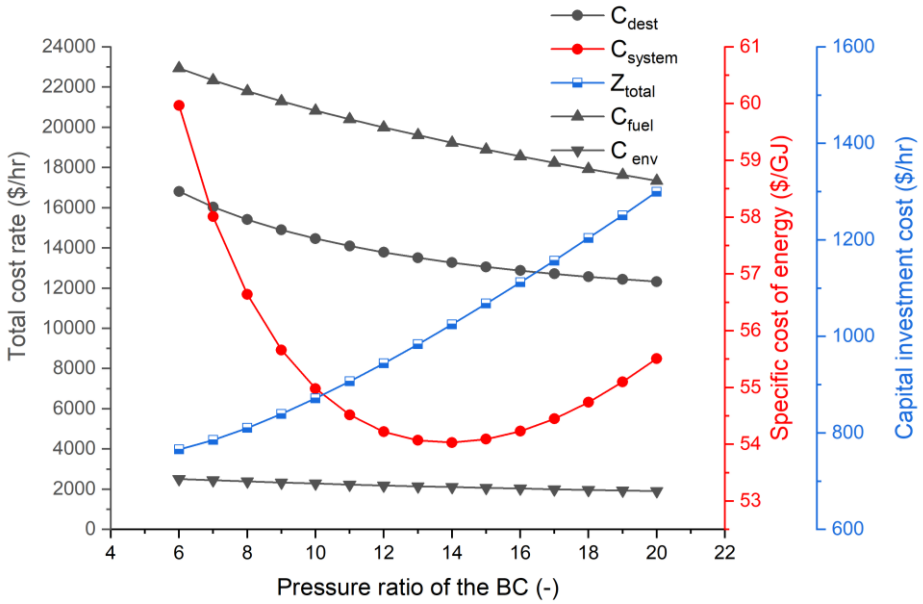

Figure 4.2. Effects of the BC’s pressure ratio on the total cost rate, the specific cost of energy, and the capital investment rate.

Figure 4.3 elucidates the impact of the BC’s pressure ratio on the combined cycle's overall performance metrics, encompassing efficiency, CO_2 emissions, and exhaust CO_2 mass flow rate. The analysis reveals a direct correlation between the BC’s pressure ratio and the combined cycle's overall efficiency. Interestingly, an increase in the BC pressure ratio leads to a concomitant decrease in both the total power output and the fuel consumption of the cycle. While the reduction in power output might initially appear counterintuitive, the decrease in fuel consumption is demonstrably more significant. This translates to lower energy and exergy inputs into the system, ultimately resulting in enhanced overall efficiencies for the combined cycle. As depicted in the figure, the designed system achieves its peak thermal and exergy efficiencies of 40.73% and 39.33%, respectively, at a BC’s pressure ratio of 16 bar. Furthermore, the decline in fuel consumption associated with an increased BC’s

pressure ratio also leads to a reduction in the CO_2 mass flow rate at the exhaust, resulting in lower CO_2 emissions. The data reveals a significant decrease in CO_2 emissions, dropping from 525.3 kg CO_2/MWh to 481.1 kg CO_2/MWh as the BC's pressure ratio increases from 6 to 20.

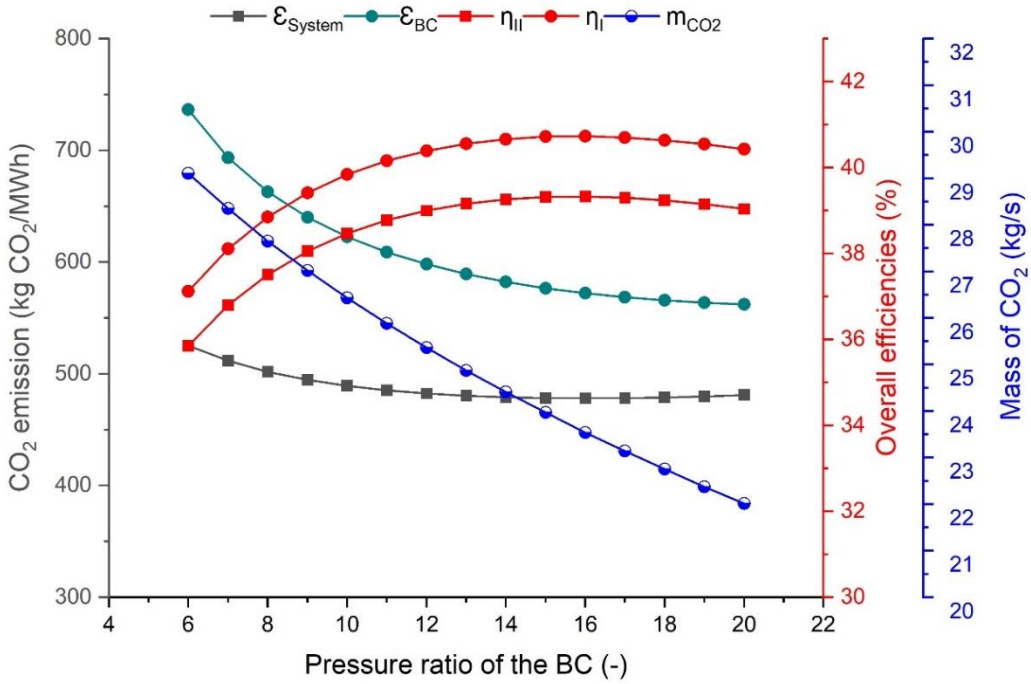

Figure 4.3. Effects of the BC's pressure ratio on the overall efficiencies of the combined cycle, the CO_2 emission, the mass flow rate of the CO_2 in the exhaust.

Figure 4.4 demonstrates how the GTIT influences various main parameters: the power generated by the BC cycle itself, the power output of the ORC, the total power output of the overall system, and the cooling load of the ARC. An increase in the GTIT leads to higher power generation by both the GT and the ORC. This effect is attributed to the GTIT raising the exhaust temperature of the gas turbine, thereby increasing the amount of energy available for the ORC cycle to exploit. Consequently, this causes an increase in the ORC's mass flow rate, which enhances its power generation capabilities and contributes to an overall improvement in the power output and efficiency of the entire cycle. As shown in Figure 4.4, raising the GTIT results in a significant increase in the total system's net power output, from 166.8 MW to 274.8 MW. The findings further demonstrate that the system's cooling capacity remains constant at 35.9 MW

as the GTIT is raised from 1300 K to 1575 K. This stability is due to the energy input to the ARC's generator remaining adequate to sustain this level of cooling output.

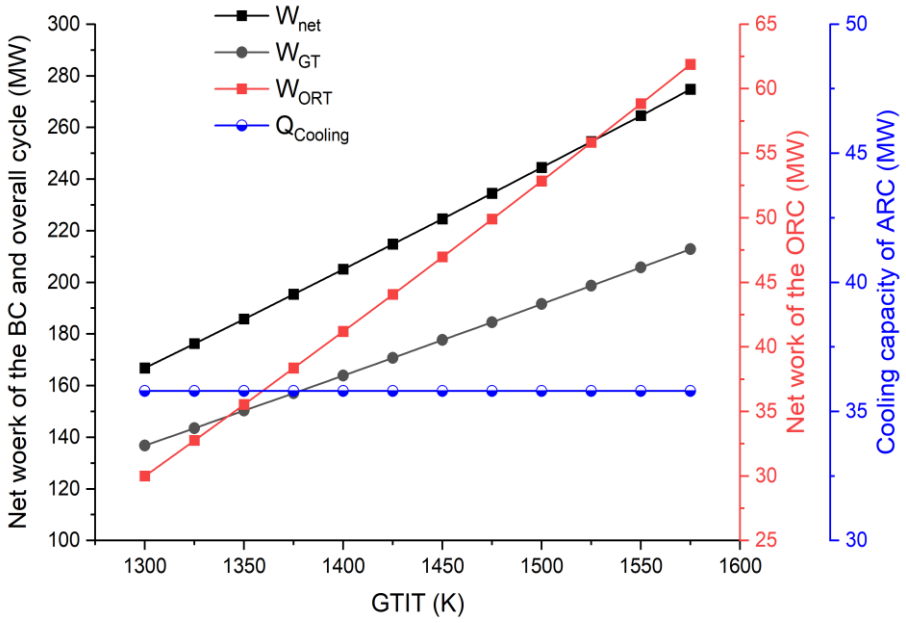

Figure 4.4. Effects of the GTIT on the BC cycle's net power output, ORC's net power output, overall system's net power output, and ARC's cooling load.

The influence of the GTIT on the total cost rate, energy cost per unit, and capital investment requirements are illustrated in Figure 4.5. The figure shows that fuel and environmental costs escalate with increased GTIT. The cost rise is directly related to the augmented fuel consumption and CO_2 emissions accompanying a higher GTIT, consequently elevating fuel and environmental expenses. Specifically, as detailed in Figure 4.5, a hike in the GTIT results in fuel costs climbing from \$18,587 to \$27,202 per hour and environmental costs increasing from 2,037 USD/hr to 2,982 USD/hr. The figure further demonstrates that both the cost of exergy destruction and the capital investment cost rise with an increase in the GTIT. The capital investment costs for the combustion chamber (CC) and gas turbine (GT) are directly tied to the GTIT, showing a significant uptick at higher GTIT values. The energy cost per unit initially falls to a minimum before it increases again with further increases in the GTIT. This trend is associated with the heightened fuel and exergy destruction costs at increased GTIT levels, leading to a higher cost per unit of energy. The figure highlights that the most economically specific energy cost, at 50.85 \$/GJ, is achieved at a GTIT of 1525 K.

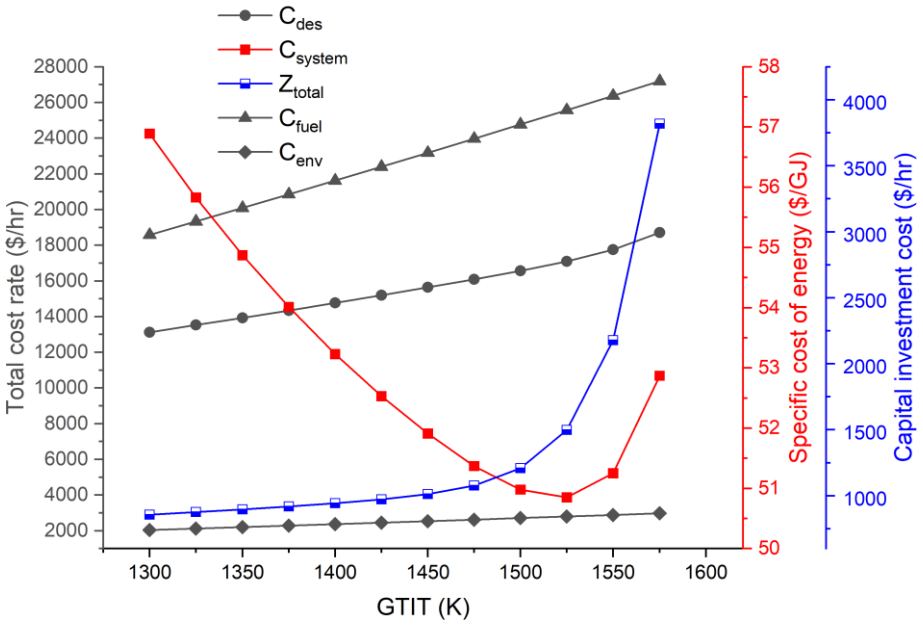

Figure 4.5. Effects of the GTIT on the total cost rate, the specific cost of energy, and the capital investment rate.

Figure 4.6 demonstrates the effects of increasing the GTIT on the combined cycle's efficiencies, CO_2 emissions, and the exhaust's CO_2 mass flow rate. Contrary to initial expectations, as the GTIT rises, the overall efficiencies of the combined cycle improve instead of diminishing. This improvement is due to the simultaneous increase in the cycle's total power output and fuel consumption accompanying higher GTIT levels. The elevated fuel consumption leads to increased energy and exergy inputs into the system, balanced by the enhanced total power output, boosting the system's overall efficiencies. Specifically, as the GTIT increases from 1300 K to 1575 K, there's an upturn in thermal efficiency from 38.77% to 43.64%, and exergy efficiency climbs from 37.43% to 42.14%. Moreover, while the CO_2 mass flow rate at the exhaust increases with higher GTIT values, CO_2 emissions for both the BC and the overall system actually decrease. This decrease is linked to the augmented total power output driven by the higher GTIT, which offsets the CO_2 mass flow rate rise. Accordingly, CO_2 emissions drop from 620.5 kg CO2/MWh to 583.5 kg CO_2/MWh for the BC and from 501.9 kg CO2/MWh to 484.3 kg CO_2/MWh for the overall system.

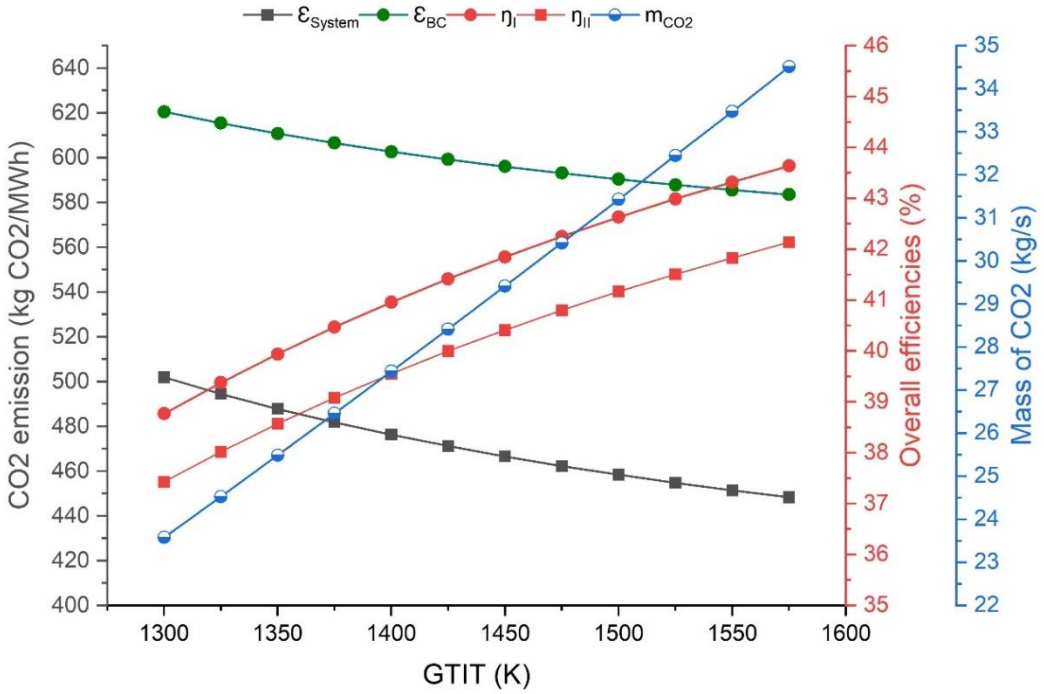

Figure 4.6. Effects of the GTIT on the overall efficiencies of the combined cycle, the CO_2 emission, the mass flow rate of the CO_2 in the exhaust.

Figure 4.7 illustrates the influence of the organic Rankine cycle turbine Inlet temperature (ORTIT) on key parameters of the combined cycle system. These parameters include the BC's power output, the ORC's power output, the total system power output, and the ARC’s cooling load. The figure illustrates d that BC’s power output remains constant while the ORC's power output increases with an increase in the ORTIT. The observed enhancement can be ascribed to the ORTIT elevating the enthalpy of the working fluid at the ORC turbine inlet. This translates to a greater availability of energy for the ORC cycle to utilize, ultimately contributing to an overall rise in the power output and efficiency of the combined cycle. Examining Figure 4.7 reveals that BC maintains a steady power output of 153 MW. In contrast, the ORC demonstrates a noteworthy rise in power output from 33.74 MW to 36.66 MW as the ORTIT increases from 560 K to 600 K. This translates to a corresponding increase in the total net power output of the entire system, rising from 186.7 MW to 189.6 MW. The impact of ORTIT on the system's cooling capacity, as evidenced by the current data, is similar to the impact of the GTIT.

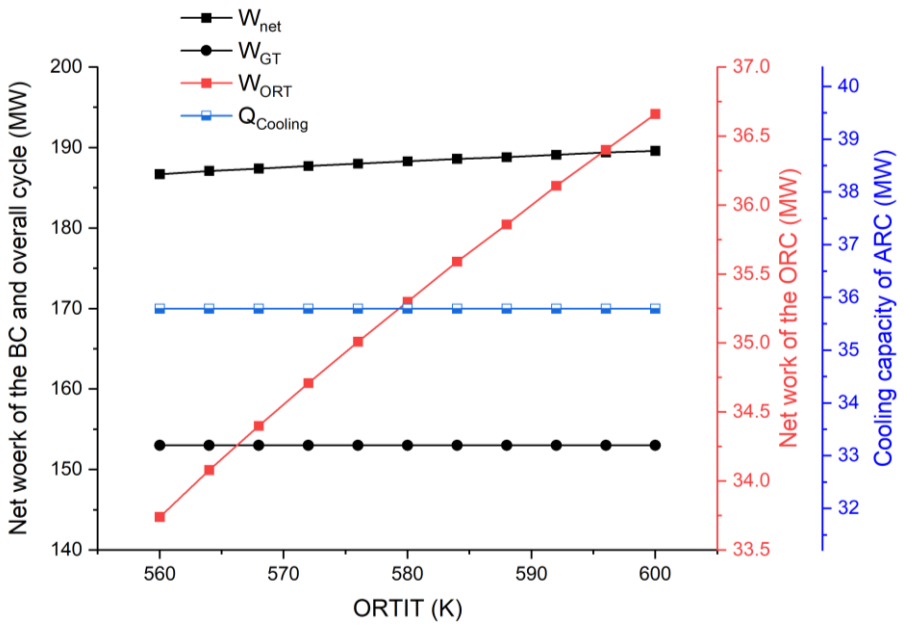

Figure 4.7. Effects of the ORTIT on the net power output of BC cycle, the net power output of ORC, the net power output of the overall system, and the cooling load of the ARC.

As depicted in Figure 4.8, increasing the ORTIT has a multifaceted impact on the system's economic performance. While fuel and environmental costs remain largely unaffected, a slight reduction in both exergy destruction costs and capital investment needs is observed. Additionally, the energy cost per unit exhibits a diminishing downward trend with rising ORTIT. The data reveals a decrease in energy cost per unit from 55.81 USD/hr to 54.52 USD/hr as the ORTIT increases from 560 K to 600 K.

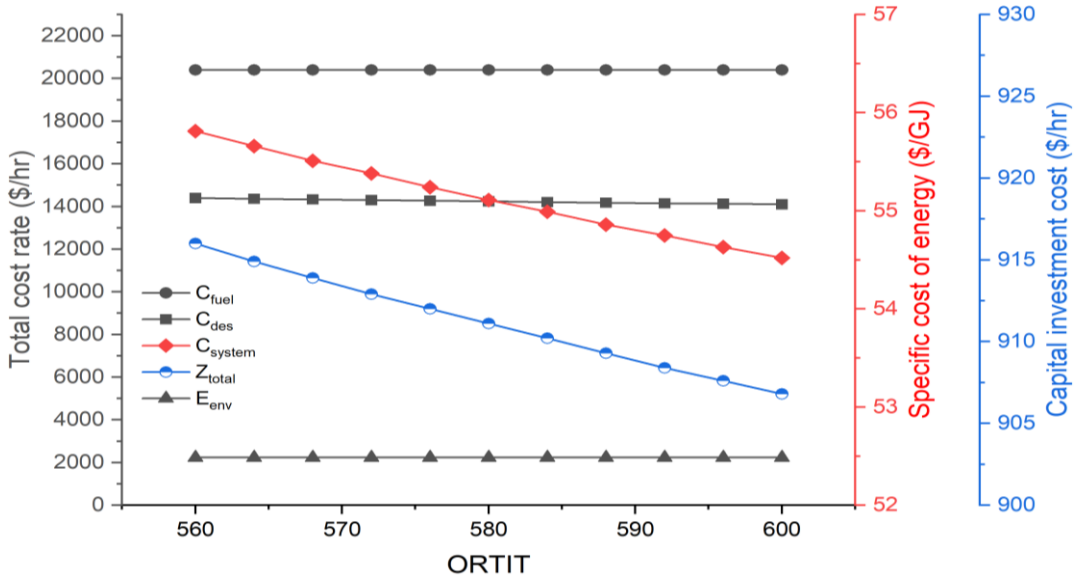

Figure 4.8. Effects of the GTIT on the total cost rate, the specific cost of energy, and the capital investment rate.

Figure 4.9 displays the effects of the ORTIT) on the combined cycle's overall efficiencies, CO_2 emissions, and CO_2 mass flow rate at the exhaust. The findings illustrate that an increase in the ORTIT leads to a marginal enhancement in the combined cycle's overall efficiencies, attributed to a slight rise in the cycle's total power output. The data demonstrate that as the ORTIT moves from 560 K to 600 K, thermal efficiency rises from 39.54% to 40.16%, and exergy efficiency increases from 38.18% to 38.78%. Moreover, the figure showed that the CO_2 mass flow rate at the exhaust stays unchanged as the ORTIT increases, and the CO_2emissions for the BC also remain steady. However, there's a minor decrease in CO_2 emissions for the entire system, a change linked to the boost in the cycle's total power output accompanying an increase in the ORTIT. The data reveals that as the ORTIT is raised from 560 K to 600 K, CO_2 emissions for the overall system decrease from 492.8 kg CO_2/MWh to 485.3 kg CO_2/MWh, whereas for the BC, it stays constant at 609 kg CO_2/MWh.

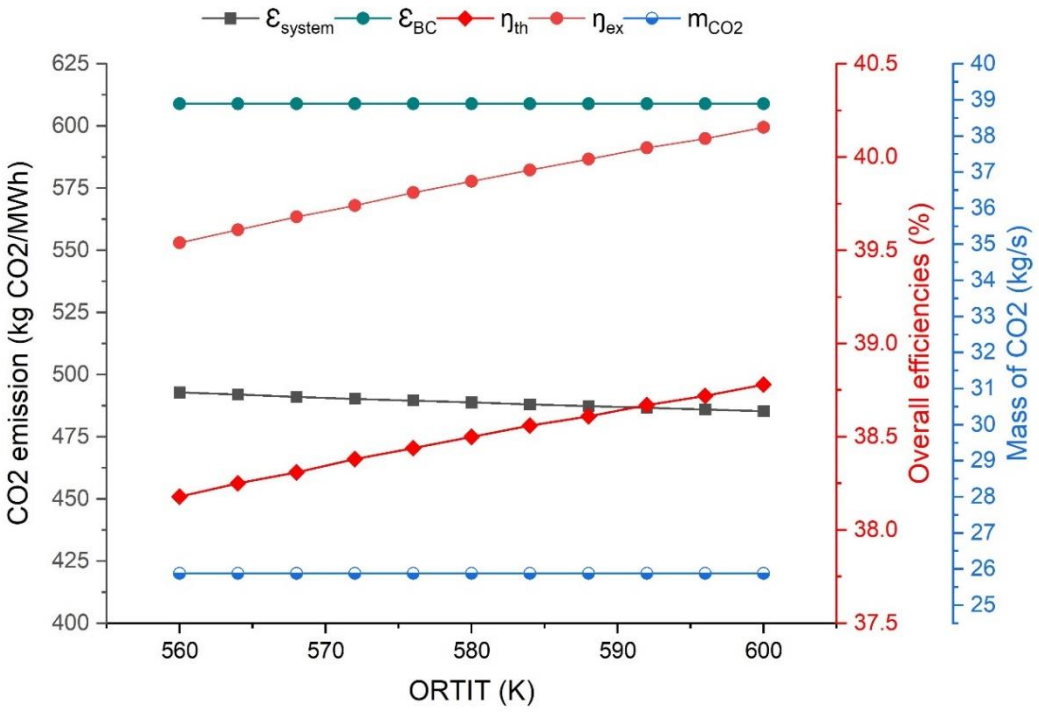

Figure 4.9. Effects of the ORTIT on the overall efficiencies of the combined cycle, the CO_2 emission, the mass flow rate of the CO_2 in the exhaust.

PART 5

CONCLUSION

This thesis introduces a hybrid power system composed of a gas turbine, an Organic Rankine Cycle (ORC), and an absorption refrigeration system (ARS) specifically designed for operation in the Marib, Yemen region. The system is expertly crafted to adhere to all necessary operational specifications. Its innovative design allows waste heat recovery, aiming to minimize thermal losses, enhance overall system efficiency, and lower operational costs. Additionally, a comprehensive 4E (energy, exergy, economic, and environmental) analysis is conducted to assess the impact of various parameters on the system's performance. The Engineering Equation Solver (EES) software is utilized to develop the model employed in this research. The following are the primary findings from this study:

- Under ideal conditions, a Bottoming Cycle (BC) can generate around 153 MW. Incorporating the ORC cycle improves the cycle's net output power by 36.66 MW, resulting in a combined system net power output of around 189.6 MW. In addition, the absorption refrigeration system can produce 35.8 MW of cooling with a COP of 0.81. The hybrid system's calculated energetic and exergetic efficiencies are 40.16% and 38.9%, respectively.
- The exergoeconomic analysis of the hybrid system revealed that the overall cost rate is 38553.18 USD/hour. This includes fuel consumption at 52.5%, capital investment at 2.5%, exergy destruction at 38.8%, and environmental costs at 5.8%. The exergoeconomic factor is calculated at 6.07%, and the unit cost of specific energy for the hybrid system amounts to 54.52 USD/GJ.
- The environmental assessment discovered that the carbon footprint of the Brayton cycle amounted to 631 kg/MWh, which decreased to 485.5 kg/MWh by adopting a hybrid system. This significant reduction in carbon emissions

highlights the effectiveness of harnessing waste heat from the Brayton cycle for environmental improvement.

- Among the various parameters evaluated, those associated with the gas turbine cycle, such as the BC's pressure ratio and GTIT, exert the most significant influence on the overall system performance. This is attributed to the gas turbine cycle functioning as the primary cycle, where any modifications can impact the entire system's efficiency.
- Raising the BC's pressure ratio reduces net output power while significantly boosting the hybrid system's energy and exergy efficiencies. Conversely, the impact of increasing the GTIT contrasts with that of the BC's pressure ratio; elevating the GTIT enhances both the net output power and the energy and exergy efficiencies of the hybrid system.
- Increasing the BC's pressure ratio and GTIT initially reduces the energy cost per unit to its lowest point, after which the cost begins to rise with further increments in these parameters. The minimum specific energy cost is observed at 54.03 $/GJ when the pressure ratio reaches 14 bar. Additionally, the most cost-effective specific energy cost, at 50.85 $/GJ, is attained at a GTIT of 1525 K.
- Elevating the BC’s pressure ratio proved to be environmentally advantageous by lowering CO_2 emissions. Conversely, the impact of raising the GTIT contrasts with that of the BC's pressure ratio; an increase in the GTIT leads to higher CO_2 emissions.

Elevating the ORTIT leads to a slight improvement in both the net output power and the energy and exergy efficiencies of the hybrid system.

REFERENCES

1. Kong, X. and Li, Y., "Design and Assessment of CCHP Systems", Handbook of Energy Systems in Green Buildings, ***Springer Berlin Heidelberg***, Berlin, Heidelberg, 1–40 (2017).

2. Safaei, S., Keynia, F., Haghdady, S., Heydari, A., and Lamagna, M., "Design of CCHP System with the Help of Combined Chiller System, Solar Energy, and Gas Microturbine", (2023).

3. Bayendang, N. P., Kahn, M. T., and Balyan, V., "Combined cold, heat and power (CCHP) systems and fuel cells for CCHP applications: a topological review", ***Clean Energy***, 7 (2): 436–491 (2023).

4. Rostamzadeh, H., Ebadollahi, M., Ghaebi, H., and Shokri, A., "Comparative study of two novel micro-CCHP systems based on organic Rankine cycle and Kalina cycle", ***Energy Conversion And Management***, 183: 210–229 (2019).

5. Petchers, N., "Combined Heating, Cooling & Power Handbook: Technologies & Applications", ***River Publishers***, (2012).

6. Li, Y. and Kong, X., "Introduction to CCHP Systems", Handbook of Energy Systems in Green Buildings, ***Springer Berlin Heidelberg***, Berlin, Heidelberg, 551–572 (2018).

7. Chu, X., Yang, D., and Li, J., "Sustainability assessment of combined cooling, heating, and power systems under carbon emission regulations", ***Sustainability***, 11 (21): 5917 (2019).

8. Salimi, M., Hosseinpour, M., Mansouri, S., and N. Borhani, T., "Environmental aspects of the combined cooling, heating, and power (CCHP) systems: a review", ***Processes***, 10 (4): 711 (2022).

9. Wegener, M., Malmquist, A., Isalgué, A., and Martin, A., "Biomass-fired combined cooling, heating and power for small scale applications–A review", ***Renewable And Sustainable Energy Reviews***, 96: 392–410 (2018).

10. Bayendang, N. P., Kahn, M. T., and Balyan, V., "Combined cold, heat and power (CCHP) systems and fuel cells for CCHP applications: a topological review", ***Clean Energy***, 7 (2): 436–491 (2023).

11. Maraver, D., Sin, A., Royo, J., and Sebastián, F., "Assessment of CCHP systems based on biomass combustion for small-scale applications through a review of the technology and analysis of energy efficiency parameters", ***Applied Energy***, 102: 1303–1313 (2013).

12. Yunus A Çengel, "Thermodynamics: An Engineering Approach", Angewandte Chemie International Edition, 6(11), 951–952., 2013–2015 (2003).

13. Wettstein, H. E., "80 years open GT development in Baden", (2019).

14. Kareem, A. F., Akroot, A., Abdul Wahhab, H. A., Talal, W., Ghazal, R. M., and Alfaris, A., "Exergo–Economic and Parametric Analysis of Waste Heat Recovery from Taji Gas Turbines Power Plant Using Rankine Cycle and Organic Rankine Cycle", ***Sustainability (Switzerland)***, 15 (12): (2023).

15. Boyce, M. P., "Gas Turbine Engineering Handbook", ***Elsevier***, (2011).

16. Talal, W. and Akroot, A., "Exergoeconomic Analysis of an Integrated Solar Combined Cycle in the Al-Qayara Power Plant in Iraq", ***Processes***, 11 (3): (2023).

17. Saravanamuttoo, H. I. H., Rogers, G. F. C., and Cohen, H., "Gas Turbine Theory", ***Pearson Education***, (2001).

18. Talal, W. and Akroot, A., "An Exergoeconomic Evaluation of an Innovative Polygeneration System Using a Solar-Driven Rankine Cycle Integrated with the Al-Qayyara Gas Turbine Power Plant and the Absorption Refrigeration Cycle", ***Machines***, 12 (2): 133 (2024).

19. Quoilin, S. and Lemort, V., "Technological and economical survey of organic Rankine cycle systems", (2009).

20. Bdaiwi, M., Akroot, A., Wahhab, H. A. A., and Mahariq, I., "Numerical analysis of the steam turbine performance in power station with a low power cycle", (2023).

21. Tchanche, B. F., Lambrinos, G., Frangoudakis, A., and Papadakis, G., "Low-grade heat conversion into power using organic Rankine cycles–A review of various applications", ***Renewable And Sustainable Energy Reviews***, 15 (8): 3963–3979 (2011).

22. Saleh, B., Koglbauer, G., Wendland, M., and Fischer, J., "Working fluids for low-temperature organic Rankine cycles", ***Energy***, 32 (7): 1210–1221 (2007).

23. Lecompte, S., Huisseune, H., Van Den Broek, M., Vanslambrouck, B., and De Paepe, M., "Review of organic Rankine cycle (ORC) architectures for waste heat recovery", ***Renewable And Sustainable Energy Reviews***, 47: 448–461 (2015).

24. Quoilin, S., Van Den Broek, M., Declaye, S., Dewallef, P., and Lemort, V., "Techno-economic survey of Organic Rankine Cycle (ORC) systems", ***Renewable And Sustainable Energy Reviews***, 22: 168–186 (2013).

25. Quoilin, S., Orosz, M., Hemond, H., and Lemort, V., "Performance and design optimization of a low-cost solar organic Rankine cycle for remote power generation", ***Solar Energy***, 85 (5): 955–966 (2011).

26. Franco, A. and Russo, A., "Combined cycle plant efficiency increase based on the optimization of the heat recovery steam generator operating parameters", ***International Journal Of Thermal Sciences***, 41 (9): 843–859 (2002).

27. Razmi, A., Soltani, M., and Torabi, M., "Investigation of an efficient and environmentally-friendly CCHP system based on CAES, ORC and compression-absorption refrigeration cycle: Energy and exergy analysis", ***Energy Conversion And Management***, 195: 1199–1211 (2019).

28. Buonomano, A., Calise, F., Ferruzzi, G., and Vanoli, L., "A novel renewable polygeneration system for hospital buildings: Design, simulation and thermo-economic optimization", ***Applied Thermal Engineering***, 67 (1–2): 43–60 (2014).

29. Świerzewski, M. and Kalina, J., "Optimisation of biomass-fired cogeneration plants using ORC technology", ***Renewable Energy***, 159: 195–214 (2020).

30. Herold, K. E., Radermacher, R., and Klein, S. A., "Absorption Chillers and Heat Pumps", ***CRC Press***, (2016).

31. Khudhur, J., Akroot, A., and Al-samari, A., "Experimental Investigation of Direct Solar Photovoltaics that Drives Absorption Refrigeration System", ***Journal Of Advanced Research In Fluid Mechanics And Thermal Sciences***, 1 (1): 116–135 (2023).

32. Hwang, Y., Radermacher, R., Alili, A. Al, and Kubo, I., "Review of solar cooling technologies", ***Hvac&R Research***, 14 (3): 507–528 (2008).

33. Sarbu, I. and Sebarchievici, C., "Review of solar refrigeration and cooling systems", ***Energy And Buildings***, 67: 286–297 (2013).

34. Huang, Z., You, H., Chen, D., Hu, B., Liu, C., Xiao, Y., Prokazov, A., and Lysyakov, A., "Thermodynamic, economic, and environmental analyses and multi-objective optimization of a CCHP system based on solid oxide fuel cell and gas turbine hybrid power cycle", ***Fuel***, 368: 131649 (2024).

35. Du, J. and Guo, J., "Analysis of multi-cascade CCHP system with gas turbine bypass extraction air energy storage", ***Applied Thermal Engineering***, 232: 121021 (2023).

36. Lucarelli, G., Genovese, M., Florio, G., and Fragiacomo, P., "3E (energy, economic, environmental) multi-objective optimization of CCHP industrial plant: Investigation of the optimal technology and the optimal operating strategy", ***Energy***, 278: 127837 (2023).

37. Wang, A., Wang, S., Ebrahimi-Moghadam, A., Farzaneh-Gord, M., and Moghadam, A. J., "Techno-economic and techno-environmental assessment and multi-objective optimization of a new CCHP system based on waste heat recovery from regenerative Brayton cycle", ***Energy***, 241: 122521 (2022).

38. Norani, M. and Deymi-Dashtebayaz, M., "Energy, exergy and exergoeconomic optimization of a proposed CCHP configuration under two different operating scenarios in a data center: Case study", ***Journal Of Cleaner Production***, 342: 130971 (2022).

39. Liu, Y., Han, J., and You, H., "Exergoeconomic analysis and multi-objective optimization of a CCHP system based on SOFC/GT and transcritical CO2 power/refrigeration cycles", ***Applied Thermal Engineering***, 230: 120686 (2023).

40. Nondy, J. and Gogoi, T. K., "4E analyses of an intercooled-recuperative gas turbine-based CCHP system: Parametric analysis and tri-objective optimization", ***Thermal Science And Engineering Progress***, 39: 101719 (2023).

41. Jia, J., Zang, G., and Paul, M. C., "Energy, exergy, and economic (3E) evaluation of a CCHP system with biomass gasifier, solid oxide fuel cells, micro-gas turbine, and absorption chiller", ***International Journal Of Energy Research***, 45 (10): 15182–15199 (2021).

42. Lei, H., Yang, J., Tang, C., and Han, D., "Energy and, exergy analysis of a CCHP-ORC system based on MGT–ORC and absorption chiller", ***Environmental Progress & Sustainable Energy***, 37 (4): 1513–1522 (2018).

43. Chahartaghi, M., Namdarian, R., Hashemian, S. M., Malek, R., and Hashemi, S., "Energy, exergy, economic, and environmental (4E) analyses and optimization of a CCHP system with steam turbine", ***Energy Science & Engineering***, 9 (6): 897–915 (2021).

44. Zeng, R., Gan, J., Guo, B., Zhang, X., Li, H., Yin, W., and Zhang, G., "Thermodynamic performance analysis of solid oxide fuel cell-combined cooling, heating and power system with integrated supercritical CO2 power cycle-organic Rankine cycle and absorption refrigeration cycle", ***Energy***, 283: 129133 (2023).

45. Hai, T., Alsubai, S., Yahya, R. O., Gemeay, E., Sharma, K., Alqahtani, A., and Alanazi, A., "Multiobjective optimization of a cogeneration system based on gas turbine, organic rankine cycle and double-effect absorbtion chiller", ***Chemosphere***, 338: 139371 (2023).

46. Wang, Q., Duan, L., Lu, Z., and Zheng, N., "Thermodynamic and economic analysis of a multi-energy complementary distributed cchp system coupled with solar thermochemistry and active energy storage regulation process", ***Energy Conversion And Management***, 292: 117429 (2023).

47. García-Domínguez, J., Blanco-Marigorta, A. M., and Marcos, J. D., "Analysis of a solar driven ORC-absorption based CCHP system from a novel exergy approach", ***Energy Conversion And Management: X***, 19: 100402 (2023).

48. Musharavati, F., Khanmohammadi, S., Pakseresht, A. H., and Khanmohammadi, S., "Enhancing the performance of an integrated CCHP

system including ORC, Kalina, and refrigeration cycles through employing TEG: 3E analysis and multi-criteria optimization", ***Geothermics***, 89: 101973 (2021).

49. Nazari, N., Mousavi, S., and Mirjalili, S., "Exergo-economic analysis and multi-objective multi-verse optimization of a solar/biomass-based trigeneration system using externally-fired gas turbine, organic Rankine cycle and absorption refrigeration cycle", ***Applied Thermal Engineering***, 191: 116889 (2021).

50. Asgari, N., Saray, R. K., and Mirmasoumi, S., "Energy and exergy analyses of a novel seasonal CCHP system driven by a gas turbine integrated with a biomass gasification unit and a LiBr-water absorption chiller", ***Energy Conversion And Management***, 220: 113096 (2020).

51. Wang, S., Liu, C., Li, J., Sun, Z., Chen, X., and Wang, X., "Exergoeconomic analysis of a novel trigeneration system containing supercritical CO2 Brayton cycle, organic Rankine cycle and absorption refrigeration cycle for gas turbine waste heat recovery", ***Energy Conversion And Management***, 221: 113064 (2020).

52. Abd El-Sattar, H., Kamel, S., Vera, D., and Jurado, F., "Tri-generation biomass system based on externally fired gas turbine, organic rankine cycle and absorption chiller", ***Journal Of Cleaner Production***, 260: 121068 (2020).

53. Zare, V. and Takleh, H. R., "Novel geothermal driven CCHP systems integrating ejector transcritical CO2 and Rankine cycles: Thermodynamic modeling and parametric study", ***Energy Conversion And Management***, 205: 112396 (2020).

54. Parikhani, T., Azariyan, H., Behrad, R., Ghaebi, H., and Jannatkhah, J., "Thermodynamic and thermoeconomic analysis of a novel ammonia-water mixture combined cooling, heating, and power (CCHP) cycle", ***Renewable Energy***, 145: 1158–1175 (2020).

55. Zhang, F., Liao, G., Jiaqiang, E., Chen, J., Leng, E., and Sundén, B., "Thermodynamic and exergoeconomic analysis of a novel CO2 based combined cooling, heating and power system", ***Energy Conversion And Management***, 222: 113251 (2020).

56. Saini, P., Singh, J., and Sarkar, J., "Thermodynamic, economic and environmental analyses of a novel solar energy driven small-scale combined cooling, heating and power system", ***Energy Conversion And Management***, 226: 113542 (2020).

57. Razmi, A., Soltani, M., and Torabi, M., "Investigation of an efficient and environmentally-friendly CCHP system based on CAES, ORC and compression-absorption refrigeration cycle: Energy and exergy analysis", ***Energy Conversion And Management***, 195: 1199–1211 (2019).

58. Zhang, X., Zeng, R., Deng, Q., Gu, X., Liu, H., He, Y., Mu, K., Liu, X., Tian, H., and Li, H., "Energy, exergy and economic analysis of biomass and

geothermal energy based CCHP system integrated with compressed air energy storage (CAES)", ***Energy Conversion And Management***, 199: 111953 (2019).

59. Moghimi, M., Emadi, M., Ahmadi, P., and Moghadasi, H., "4E analysis and multi-objective optimization of a CCHP cycle based on gas turbine and ejector refrigeration", ***Applied Thermal Engineering***, 141: 516–530 (2018).

60. Mehrpooya, M., Ghorbani, B., and Hosseini, S. S., "Thermodynamic and economic evaluation of a novel concentrated solar power system integrated with absorption refrigeration and desalination cycles", ***Energy Conversion And Management***, 175: 337–356 (2018).

61. Eisavi, B., Khalilarya, S., Chitsaz, A., and Rosen, M. A., "Thermodynamic analysis of a novel combined cooling, heating and power system driven by solar energy", ***Applied Thermal Engineering***, 129: 1219–1229 (2018).

62. Moghimi, M., Emadi, M., Akbarpoor, A. M., and Mollaei, M., "Energy and exergy investigation of a combined cooling, heating, power generation, and seawater desalination system", ***Applied Thermal Engineering***, 140: 814–827 (2018).

63. Nondy, J. and Gogoi, T. K., "4E analyses of an intercooled-recuperative gas turbine-based CCHP system: Parametric analysis and tri-objective optimization", ***Thermal Science And Engineering Progress***, 39: (2023).

64. Akroot, A. and Namli, L., "Performance assessment of an electrolyte-supported and anode-supported planar solid oxide fuel cells hybrid system", ***J Ther Eng***, 7 (7): 1921–1935 (2021).

65. Akroot, A., "Effect of Operating Temperatures on the Performance of a SOFCGT Hybrid System", ***International Journal Of Trend In Scientific Research And Development***, Volume-3 (Issue-3): 1512–1515 (2019).

66. Mohammadkhani, F., Shokati, N., Mahmoudi, S. M. S., Yari, M., and Rosen, M. A., "Exergoeconomic assessment and parametric study of a Gas Turbine-Modular Helium Reactor combined with two Organic Rankine Cycles", ***Energy***, 65: 533–543 (2014).

67. Akroot, A. and Nadeesh, A., "Performance Analysis of Hybrid Solid Oxide Fuel Cell-Gas Turbine Power System", (2021).

68. Akroot, A., Namli, L., and Ozcan, H., "Compared Thermal Modeling of Anode- and Electrolyte-Supported SOFC-Gas Turbine Hybrid Systems", ***Journal Of Electrochemical Energy Conversion And Storage***, (2021).

69. J. Souza, R., Dos Santos, C. A. C., Ochoa, A. A. V., Marques, A. S., L. M. Neto, J., and Michima, P. S. A., "Proposal and 3E (energy, exergy, and exergoeconomic) assessment of a cogeneration system using an organic Rankine cycle and an Absorption Refrigeration System in the Northeast Brazil: Thermodynamic investigation of a facility case study", ***Energy Conversion And Management***, 217 (April): 113002 (2020).

70. Dhahad, H. A., Ahmadi, S., Dahari, M., Ghaebi, H., and Parikhani, T., "Energy, exergy, and exergoeconomic evaluation of a novel CCP system based on a solid oxide fuel cell integrated with absorption and ejector refrigeration cycles", ***Thermal Science And Engineering Progress***, 21 (May 2020): 100755 (2021).

71. Besevli, B., Kayabasi, E., Akroot, A., Talal, W., Alfaris, A., Assaf, Y. H., Nawaf, M. Y., Bdaiwi, M., and Khudhur, J., "Technoeconomic Analysis of Oxygen-Supported Combined Systems for Recovering Waste Heat in an Iron-Steel Facility", ***Applied Sciences***, 14 (6): 2563 (2024).

72. Nourpour, M. and Khoshgoftar Manesh, M. H., "Evaluation of novel integrated combined cycle based on gas turbine-SOFC-geothermal-steam and organic Rankine cycles for gas turbo compressor station", ***Energy Conversion And Management***, 252: (2022).

73. A Bejan, G Tsatsaronis, M. M., "Thermal Design and Optimization", Energy, 433–434 (1996).

74. Ahmadi, P. and Dincer, I., "Thermodynamic and exergoenvironmental analyses, and multi-objective optimization of a gas turbine power plant", ***Applied Thermal Engineering***, 31 (14–15): 2529–2540 (2011).

75. Tian, H., Li, R., Salah, B., and Thinh, P. H., "Bi-objective optimization and environmental assessment of SOFC-based cogeneration system: performance evaluation with various organic fluids", ***Process Safety And Environmental Protection***, 178: 311–330 (2023).

76. Akroot, A. and Al Shammre, A. S., "Techno-Economic and Environmental Impact Analysis of a 50 MW Solar-Powered Rankine Cycle System", ***Processes***, 12 (6): 1059 (2024).

RESUME

Marwan Nabil Mohammed AL-ARASHI is a mechanical engineer who graduated from the faculty of Engineering, University of Karabük – TURKEY, and obtained his bachelor's degree in 2021. He is currently studying for his master's degree at Karabük University, Department of Mechanical Engineering.